Renewable and Sustainable Energy Reviews 182 (2023) 113353

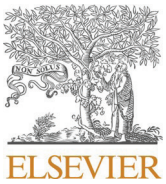

Contents lists available at ScienceDirect

Renewable and Sustainable Energy Reviews

journal homepage: www.elsevier.com/locate/rser

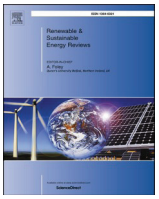

Probing the effects of hydrogen on the materials used for large-scale transport of hydrogen through multi-scale simulations

Guang Cheng [a,*], Xiaoli Wang [a], Kaiyuan Chen [a], Yang Zhang [a], T.A. Venkatesh [b,**], Xiaolin Wang [c], Zunzhao Li [c], Jing Yang [c]

[a] College of Mechanical and Electrical Engineering, Beijing University of Chemical Technology, Beijing, 100029, China
[b] Department of Materials Science and Chemical Engineering, Stony Brook University, NY, 11794, United States
[c] Sinopec Dalian Research Institute of Petroleum and Petrochemicals Co. Ltd, Dalian, 116045, China

ARTICLE INFO

Keywords:
Molecular dynamics
Density functional theory
Hydrogen compatibility
Hydrogen transportation
Multi-scale simulations

ABSTRACT

The successful realization of a hydrogen economy is crucially dependent on a comprehensive understanding of the effects of hydrogen on the hydrogen infrastructure materials and the development of hydrogen compatible materials with long term reliability. Progress made in recent times in understanding the fundamentals of hydrogen embrittlement mechanisms in metallic materials has been reviewed. Particular emphasis has been made on highlighting the challenges and breakthroughs made in the simulation of hydrogen effects across multiple length-scales using the density functional theory (DFT) method, molecular dynamics (MD) simulations and continuum approaches. The DFT approach is an important approach that provides valuable insights on the effects of hydrogen on a material due to intrinsic factors such as microstructural features and extrinsic factors such as temperature and pressure. MD simulations of hydrogen effects with new interaction potential functions that include more elements (such as Si, Mn, Cr, Ni, etc.) in models with internal defects (such as vacancies) and subjected to strain and temperature, could transform MD simulations from a mechanism studying tool to a property prediction tool. The continuum levels models have the potential to incorporate the effects of micro-structural features and predict the mechanical performance of materials, such as deformation and fatigue life under hydrogen environments. Overall, there is positive outlook for developing multi-scale computational tools for designing hydrogen compatible materials and for predicting the performance of metallic materials in hydrogen environments using a bottom-up approach.

1. Introduction

Hydrogen embrittlement has been observed as early as 1874, as can be seen in the research article of William H. Johnson [1]. The early failures due to hydrogen embrittlement happened in steels and the fracture surfaces indicated a ductile to brittle transition. The source of hydrogen could be hydrogen molecules in the natural environment which are adsorbed by the surface atoms and converted to hydrogen atoms or acidic environments which bring hydrogen atoms into the lattice structure of the materials. The interaction of hydrogen atoms with the nano/micro-structural features of a material, under external loads, promotes embrittlement which leads to premature failure at relatively lower stresses.

Several mechanisms have been proposed to explain hydrogen embrittlement such as hydrogen-enhanced decohesion (HEDE) [2–4], hydrogen-enhanced localized plasticity (HELP) [5,6], and hydrogen-enhanced strain-induced vacancy (HESIV) [7]. According to the HEDE mechanism, hydrogen atoms diffuse into the materials and reduce their cohesive strength and cracks are expected to form if the external stress exceeds the local cohesive strength. This mechanism is mainly used to explain brittle intergranular fracture. The HELP mechanism which was observed by Birnbaum and Sofronis [8–12] in aluminum, nickel and iron based materials, was initially proposed in the 1970s by Beachem [13]. According to this mechanism, no hydrides are formed and the plasticity enhancement is mainly caused by increased dislocation mobility. The HESIV mechanism was proposed based on the interaction between vacancies and hydrogen [7,14]. In this mechanism, hydrogen atoms combine with vacancies and decrease the mobility of vacancies. Subsequently, the formation of stable hydrogen

* Corresponding author.
** Corresponding author.
E-mail addresses: guangcheng@mail.buct.edu.cn (G. Cheng), t.venkatesh@stonybrook.edu (T.A. Venkatesh).

https://doi.org/10.1016/j.rser.2023.113353
Received 30 September 2022; Received in revised form 31 December 2022; Accepted 6 January 2023
Available online 20 May 2023

Nomenclature

Abbreviations

AIMD	Ab initio molecular dynamics
APT	Atom probe tomography
BCT	Body-centered tetragonal
DDD	Discrete dislocation dynamics
DFT	Density functional theory
EAM	Embedded-atom method
FCC	Face-centered cubic
FEM	Finite element method
HCP	Hexagonal close-packed
HEDE	Hydrogen-enhanced decohesion
HELP	Hydrogen-enhanced localized plasticity
HESIV	Hydrogen-enhanced strain-induced vacancy
HEVA	Hydrogen-enhanced vacancy activities
kMC	Kinetic Monte Carlo
LEAP	Local-electrode atom probe
MD	Molecular dynamics
MEAM	Modified embedded-atom method
OS	Octahedral site
PFM	Probe force microscopy
PFM	Phase field method
RVE	Representative volume element
SKPFM	Scanning Kelvin probe force microscopy
TDS	Thermal desorption spectroscopy
TS	Tetrahedral site
TEM	Transmission electron microscopy
SEM	Scanning electron microscopy
EBSD	Electron backscatter diffraction

clusters/bubbles enables rupture failure of the material.

With increased demands for a low carbon economy and reduction in carbon emissions, hydrogen, as a zero-carbon fuel has attracted plenty of interest from policymakers, industries, and academic researchers [15–17] in recent times. Hydrogen possesses a higher energy content, per unit mass 120 MJ/kg, than traditional fossil energy, such as natural gas, petroleum, or coal which can help realize the transition to a low carbon economy. However, its low volumetric energy density under normal temperature and standard atmospheric pressure (0.01 MJ/L) prevented its widespread application in the early days [18]. Hence, a moderate pressure, such as 5-20 MPa, has been adopted for the transportation of hydrogen gas in pipeline systems, and a higher pressure, such as 70 MPa, is used for hydrogen storage. Alternately, combinations of high pressures and low temperatures are used to convert gaseous hydrogen to liquid hydrogen for storage and/or transport for relatively smaller volumes of hydrogen. The possibility of hydrogen embrittlement in the materials used for storing or transporting hydrogen such as pipelines steels [19], natural gas distribution networks (with injection of hydrogen) [20], underground hydrogen storage systems [21], or cast iron and steel used in hydrogen compressors [22] poses a serious concern for the safe and economical utilization of hydrogen.

In general, transporting or storing hydrogen under high pressures would accelerate hydrogen adsorption and diffusion processes in the materials and increase the susceptibility for hydrogen embrittlement in several steel grades. However, stainless steels, such as 316L or 304L (without welded sections) are commonly and safely used for hydrogenation reactors. In principle, these stainless-steel pipelines can be used to transport high-pressure hydrogen gas. However, stainless steels are quite expensive as they generally include a high weight percentage of alloying elements, such as Ni and Cr and hence, it is not cost effective to construct large pipelines made from stainless steel. The balance between the safety and cost of the hydrogen transportation system has raised the question if low-cost materials or currently available pipeline materials can be utilized for hydrogen transport. If the pipeline materials that are currently used for transporting gases such as natural gas, are certificated as hydrogen compatible, then the existing gas transport infrastructure can be readily used to transport hydrogen.

There have been many experimental studies that have investigated hydrogen effects on the mechanical properties of metallic materials, especially, fracture toughness and strength. Several microstructural aspects such as alloying elements, composition, constituent phases, and grain structures have been correlated to the mechanical performance of the materials in hydrogen environments. Based on in-situ experiments, hydrogen pressure and temperature have been found to be two key extrinsic factors that affect the mechanical properties of materials in a significant manner. Several other studies have also investigated the effect of hydrogen charging on local microstructures and severe plastic deformation as well. These meso- and micro-scale experimental studies provide many insights on the "composition-microstructure-performance" relationships and enable suitable materials selection approaches for hydrogen transport [5,23,24]. However, experimental results often capture the cumulative effects of several intrinsic microstructural features. The effects of the individual nano/microstructural features on hydrogen embrittlement can be difficult to discern in experiments as multiple mechanisms may be activated concurrently in the materials, with some promoting embrittlement and some inhibiting embrittlement [25–27]. Hence, it is challenging to optimize the design of low cost and safe hydrogen compatible materials and manufacturing processes solely based on experimental findings.

As it is well understood that hydrogen embrittlement, which is observed at the macro-scale, is primarily caused by the atomic level phenomena associated with the diffusion and interaction of hydrogen atoms in the lattice of a material, atomistic scale simulations are well-suited for understanding the dynamics of hydrogen interactions within materials and for identifying the causative mechanisms of hydrogen embrittlement. Hence, atomistic simulations have been widely used for understanding hydrogen effects in metallic materials. In the early stages, atomistic simulations could only be utilized to solve the problems within very small volumes of material, such as those which comprise a few hundred atoms [28,29], because the computing capability could not handle large model sizes. At the present time, increased computing capability [30–32] and software or hardware-based accelerating methods have enabled the development of new atomic simulation methods for large size models. Thus, large-scale models with over 100 million atoms can be simulated, where in the elemental composition and microstructural features that are input in the model are directly obtained from various experimental methods [33–35]. For example, the mechanical properties of a small volume of material with a length-scale on the order of 100 nm can be obtained from nanoindentation or nanopillar compression experiments. With the proper interaction potentials between the metallic matrix and hydrogen, it is also possible to conduct atomistic simulations of nanoindentation to investigate the hydrogen effects and compare them with experiments, in such volumes of materials. Thus, there is a great opportunity for utilizing atomistic simulations to understand the influence of individual nano/micro-structural features. Furthermore, large-scale atomistic simulations could also provide important input data for the continuum-scale modeling as well which will help realize the multi-scale modeling approach for the bottom-up design of materials for hydrogen applications, as illustrated in Fig. 1.

Recent progress made in invoking several simulation methods to understand the effects of hydrogen in metallic materials across multiple length-scales is reviewed in this study as follows. The experimental techniques used for the direct observation of hydrogen trapping sites

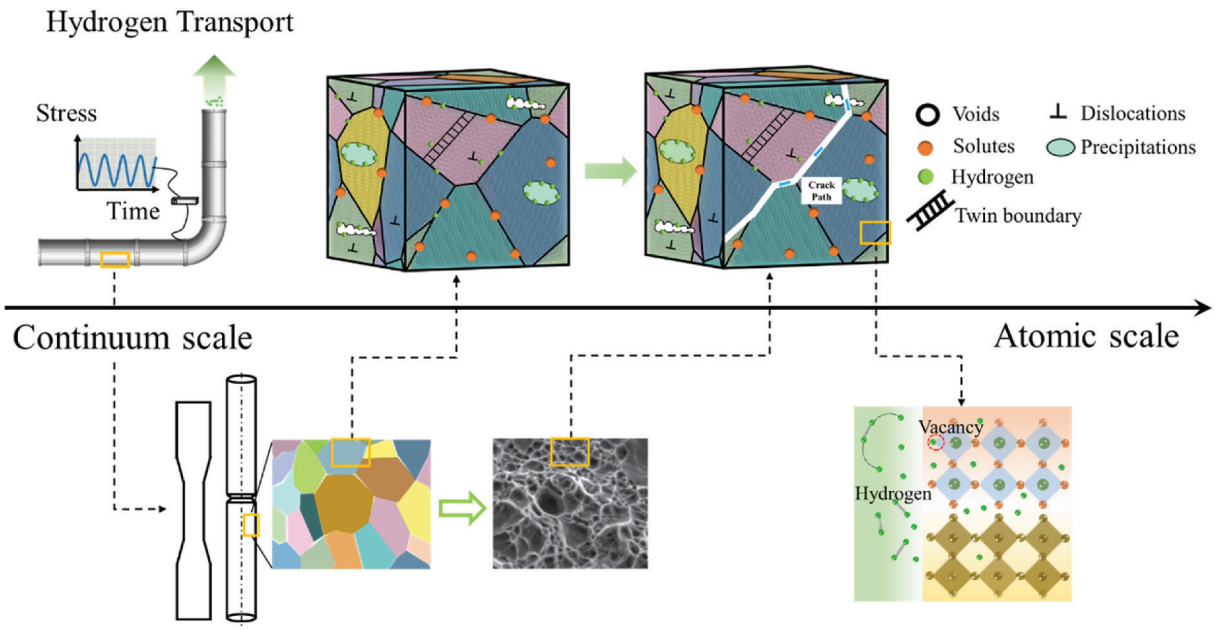

Fig. 1. The interaction between hydrogen and intrinsic features at different scales.

within the microstructures are presented in section 2. The atomistic simulations based on the density functional theory (DFT) and molecular dynamics (MD) are reviewed to elucidate the effects of the materials' intrinsic properties and extrinsic factors on hydrogen embrittlement in sections 3 and 4. Recent developments in continuum scale simulations for understanding hydrogen effects and the potential for multi-scale simulations to enable the bottom-up design of materials for hydrogen applications are discussed in section 5. Principal conclusions and the outlook for future research in invoking multi-scale modeling for understanding hydrogen embrittlement are summarized in section 6.

2. Experimental observations of hydrogen within microstructural features

In order to simulate the interactions between hydrogen and the nano/micro-structural features in a material, the experimental evaluation of the micro-structural features over multiple length-scales (as illustrated in Fig. 1) is extremely essential. Microstructural characterizations are easily obtained using several electron microscopy techniques, such as transmission electron microscopy (TEM), scanning electron microscopy (SEM), electron backscatter diffraction (EBSD), etc., and can be readily converted to digital structures in the simulation models. The total amount of trapped hydrogen can be quantified through thermal desorption spectroscopy (TDS) [36], small-angle neutron scattering [37], and energy recoil detection [38]. However, the actual trapping sites for hydrogen within the material are hard to discern. Without the information pertaining to the location of hydrogen in the material, even a large simulation model with DFT calculation or MD modeling would be either inefficient or inaccurate in investigating the effects of the trapped hydrogen in reducing strength or toughness. While the hydrogen trapping mechanism is assumed to be connected with the binding energy, a deeper understanding of the actual trapping mechanisms and the identification of the trapping sites in real microstructures would be very important. Therefore, hydrogen mapping from experiments is very crucial for developing accurate simulation models for capturing the effects of hydrogen in materials.

2.1. The atom probe tomography (APT) method

The atom probe tomography (APT) method is the main technique that is used for direct observation of hydrogen in a 100 × 100 × 1000 nm^3 three-dimensional volume, as shown in Fig. 2(a). Since it is difficult to distinguish the sample hydrogen from the background hydrogen in the ultrahigh vacuum chamber, the isotope - deuterium, is generally utilized to replace hydrogen in the sample and precision mark the trapping sites within the microstructure. The first APT work on hydrogen mapping was reported in 2002 where Kasen et al. [39] located deuterium in Pd/Ni and Fe/V multilayers. Later, Takahashi et al. directly observed H trapping in TiC and VC precipitation strengthened ferritic steel using local-electrode atom probe (LEAP) tomography. The interfaces between the matrix and TiC platelets, and misfit dislocation cores on semi-coherent platelets between the matrix and vanadium carbide (V_4C_3) were found to be dominant trapping sites and the deep trapping sites, respectively [40,41]. With the progress in sample preparation, a novel experimental configuration with liquid nitrogen was developed to keep the cold environment which helped retain deuterium in the sample during the transfer process [42]. The deuterium concentration within the steel was obtained and it was found that both the interface and the V-Mo-Nb carbides acted as trapping sites [41]. Besides the incoherent interfaces between carbide-ferrite and niobium carbide-martensite [43–45], direct observation of deuterium at carbon-rich dislocations and grain boundaries demonstrate the existence of other atomic-scale microstructural trap sites, as shown in Fig. 2(b). In addtion to the advances made in the experimental observation of ferritic steels, the LEAP method has helped to characterize the deuterium distribution in grain boundaries of ultrafine grain Al-7.5% Mg [46] and 7xx series high strength Al alloys [47].

2.2. The probe force microscopy (PFM) method

In a recent study on the high strength low alloyed martensitic steel, 316L stainless steels, and nickel, in-situ scanning Kelvin probe force microscopy (SKPFM) has been shown to have great potential in detecting hydrogen trapping near the incoherent interfaces [48–50], as illustrated in Fig. 2 (c). This contact-based measurement is found to be convenient in sample preparation and a modified Nernst equation could be used to describe the numerical relationship between the potential obtained from SKPFM and the hydrogen concentration [50]. The scanned areas with the lowest potential, such as the interfaces between the precipitate and the grains, were shown to be regions with higher

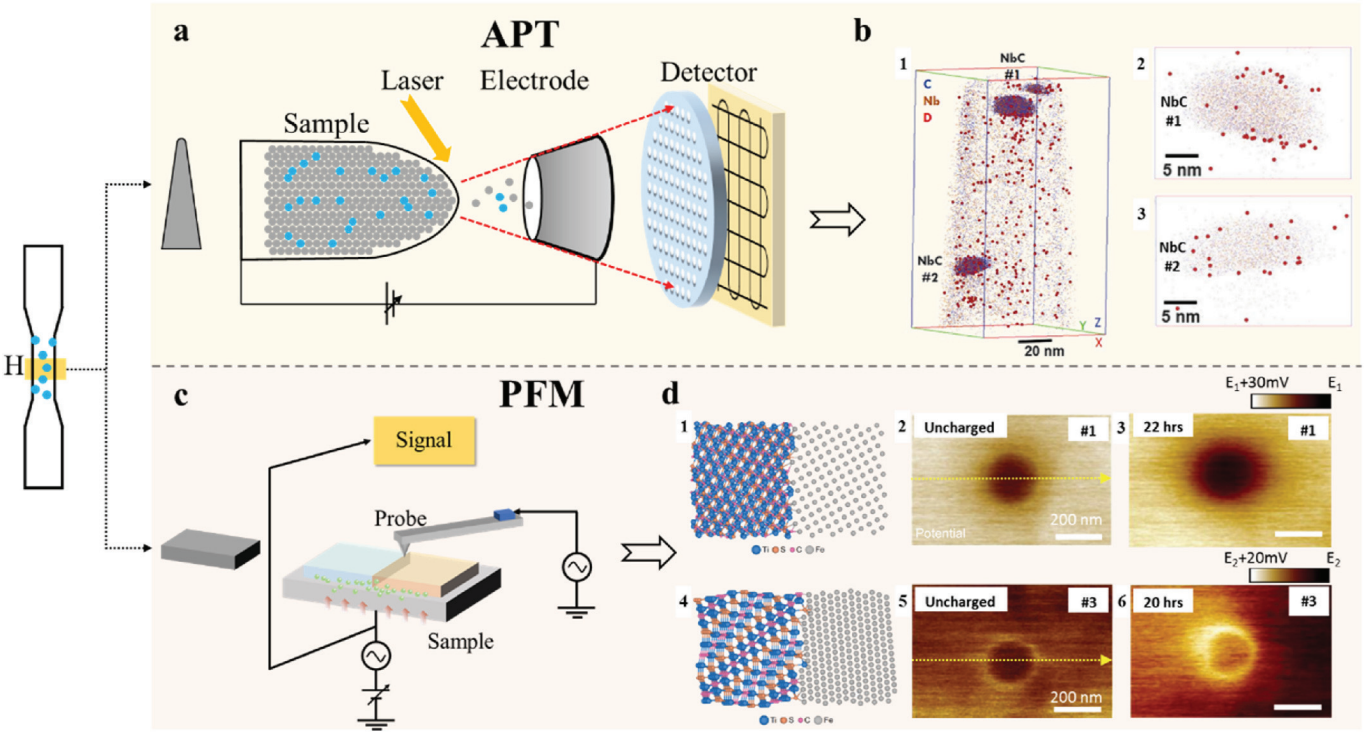

Fig. 2. Experimental observations of hydrogen within microstructures. (a) The illustration of atom probe tomography (APT) method; (b) the distribution of deuterium at a ferritic steel using APT method: (b.1) the 3D view of deuterium atoms in the sample, and 2D view of deuterium atoms near (b.2) #1 NbC precipitate, and (b.3) #2 NbC precipitate [44]; (c) the illustration of PFM method; and (d) atomic structures for two types of interface and measurement on hydrogen-precipitate interactions: (d.1) atomic structure of #1 precipitate, (d.2) potential profile of #1 precipitate before charging, (d.3) potential profile of #1 precipitate after 22 h charging, (d.4) atomic structure of #3 precipitate, (d.5) potential profile of #3 precipitate before hydrogen charging, and (d.6) potential profile of #3 precipitate after 20 h hydrogen charging [48].

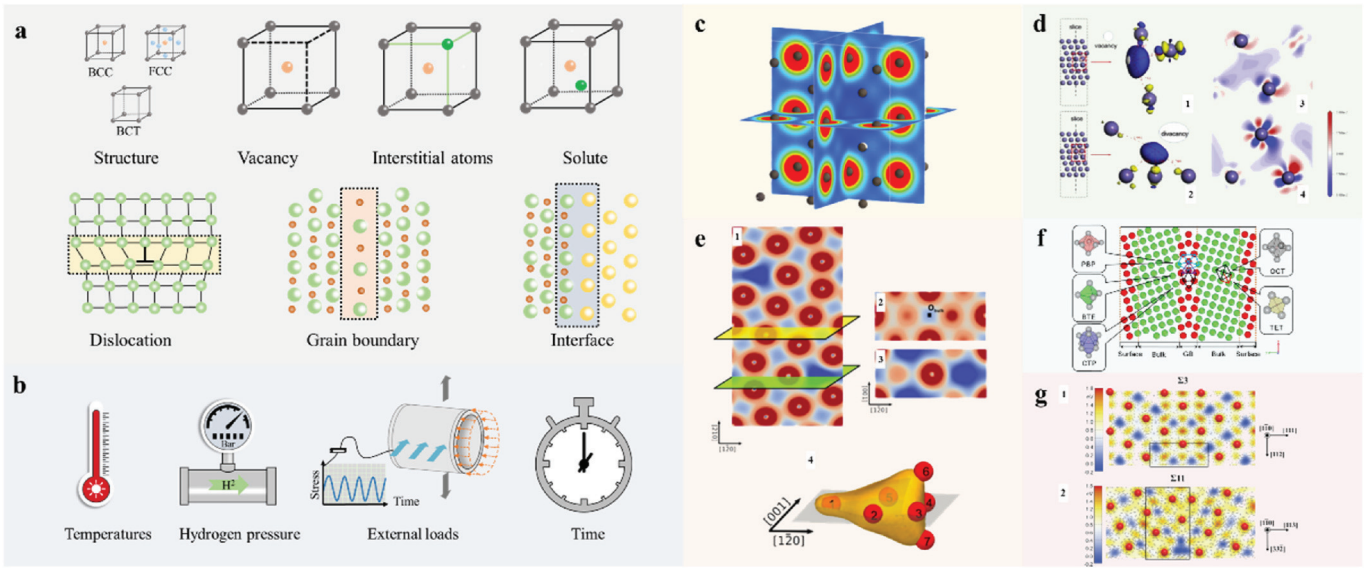

Fig. 3. The density functional theory calculations for studying hydrogen effects. (a) The intrinsic factors; (b) extrinsic factors; (c) a 53-atom BCC supercell with a vacancy at the center (The red regions denote the high potential energy zone for hydrogen atoms and the trapping sites are the dark-blue regions) [52]; (d) hydrogen atom in (d.1) single vacancy and (d.2) double-vacancy (or divacancy) of γ-Fe, and the deformation charge density of the Fe atoms across the stacking fault when hydrogen atom filled in a (d.3) single vacancy and (d.4) double-vacancy (or divacancy). (The blue and yellow denote electrons gain and depletion, respectively, in Figs. 1 and 2; and the red and blue denote electrons electron gain and depletion, respectively, in Fig. 3 and) [53]; (e) valence electron density plots for the Σ5 grain boundary in FCC Ni lattice: (e.1) the cross-sectional plane along the (0 0 1) plane, (e.2) the plane in the yellow region of Fig. 1, (e.3) the plane in the green region of Fig. 1, and (e.4) 3D structure of the grain boundary cavity as an iso-surface (Red regions denote the metastable segregation sites for hydrogen atoms) [54]; (f) the illustration of polyhedron in Ni lattice and Σ5 (130) [55] grain boundaries [56]; and (g) the potential value of (g.1) Σ3 and (g.2) Σ11 grain boundaries along the (1 $\bar{1}$ 0) plane [57].

concentration of hydrogen traps, as presented in Fig. 2 (d).

Many other studies also indicate that incoherent interfaces possess a high possibility of trapping hydrogen. Also, the lattice defects such as vacancies within the nanoprecipitates or inclusions could be hydrogen trapping sites as well. It has been shown that the incoherent precipitates with C or S vacancies serve as efficient trapping sites for hydrogen if the neighboring matrix region is under tensile strain. However, if the matrix region near the incoherent interface is under compressive strain, then the solution energy of hydrogen in that matrix region is increased which tends to exclude hydrogen from that incoherent interface [48]. Therefore, atomistic simulation using the DFT calculation and MD simulations should be invoked to provide further insights into the mechanisms of hydrogen trapping as well as hydrogen-related interactions.

3. The density functional theory calculations for studying hydrogen effects

Though deuterium could be utilized to demonstrate trapping sites in the APT-based experiments, it is to be noted that the binding energy of deuterium would be lower than that of a proton (hydrogen) because of its higher atomic mass [51]. Such subtle differences in the interatomic interactions can be captured using the density functional theory (DFT) method as it can include the specific chemical states of atomic structures, such as covalent, ionic, and metallic bonds. Thus, the binding energy and diffusion paths of hydrogen within materials have been extensively studied using DFT methods. Based on the DFT method or the data from DFT calculations, the effects of hydrogen on materials due to both the intrinsic properties (lattice structure, vacancies, interstitial atoms, substitutional solutes, dislocations, grain boundaries, and interfaces as shown in Fig. 3 (a)) and the extrinsic factors (temperatures, hydrogen pressure, external loads, and time as shown in Fig. 3 (b)) can be investigated.

3.1. DFT calculations for understanding hydrogen effects - intrinsic factors

The hydrogen-monovacancy complexes were initially studied in α-Fe [58]. The interaction between vacancy and hydrogen was confirmed to contribute to hydrogen embrittlement through the hydrogen-enhanced vacancy activities (HEVA) and increased hydrogen mobility. As summarized in Fig. 3, atomic models have been developed to study hydrogen effects in several systems such as α-Fe (body-centered cubic, BCC, as illustrated in Fig. 3 (c) [52]), γ-Fe (face-centered cubic, FCC, as illustrated in Fig. 3 (d) [53]), α′-Fe (body-centered tetragonal, BCT), ε-Fe (close-packed hexagonal, HCP) and nickel (FCC, as illustrated in Fig. 3 (e) [54]). Also, the interaction of hydrogen with grain boundaries have also been studied as illustrated in Fig. 3(e-g) [54,56,57]. There are two types of high-symmetry interstitial positions: octahedral sites (OS) and tetrahedral sites (TS) in steels [57,59,60]. It has been observed that hydrogen prefers the TS in α-Fe and α′-Fe, but OS in γ-Fe [53,60]. The energetics of hydrogen adsorption at various grain boundaries have been studied. It has been found that certain grain boundaries with higher sigma such as Σ17 and Σ73 boundaries are more capable of trapping hydrogen and thus are more prone to hydrogen embrittlement as compared to low sigma grain boundaries such as Σ3 boundaries [56]. The grain boundaries with hydrogen would lower the critical fracture strain by up to 36% according to Griffith's criterion in bcc Σ3 [57]. If the hydrogen-monovacancy complexes were formed as a cluster and accumulated at the grain boundaries, the strength of the system would be significantly reduced [61]. These calculations predict the effects of the hydrogen on the strength reduction and the results support the HEDE and HESIV mechanisms for hydrogen embrittlement.

It should be denoted that steels are more complex than pure iron because the actual lattices contain carbon, other alloy elements and some interstitial atoms [62,63]. The elements with a small radius, such as B, C, N, O, P, and S, take the interstitial positions and other alloy elements with larger sizes replace the Fe atoms in the lattice positions. Furthermore, capturing dislocations and precipitates in the DFT-based simulation is challenging.

The atomic-scale heterogeneities affect the binding energy and the diffusion paths. For example, in the Fe-Cr system hydrogen prefers the Fe-rich lattice to the Cr-rich lattice [64,65]. Recently, more elements (Co, Cr, Ni, Mn, etc.) were investigated using DFT methods and the average surface energy with H was calculated. In the complex alloy system, a lower hydrogen absorption energy would indicate a lower fracture stress, and the results were validated by the experiments with four FCC alloys, that included two stainless steels, 304L and 316L, and two high entropy alloys, Co-Cr-Fe-Ni and Co-Cr-Fe-Mn-Ni [66].

Generally, the DFT calculations provide the structure status within a short time. Kinetic Monte Carlo (kMC) simulation combined with DFT could enable longer time simulations. Hence, dislocation activity can be characterized as well. Based on the kMC with DFT data on dislocation-hydrogen interactions, the first-principles quantum mechanics-based approach and meso-scale discrete dislocation dynamics simulations have been integrated. The hydrogen-induced shear localization [67] has been numerically illustrated in a wide range of stresses and temperatures. Low external stress and low hydrogen content (such as 1 atomic parts per million, appm) were found to raise the screw dislocation mobility while hydrogen atoms within the lattice was shown to reduce the barrier and activate dislocation sources [68]. At moderate hydrogen concentrations (3-10 appm), the increase in screw dislocation mobility was not so high and at high hydrogen concentrations (20 appm) the dislocation mobility was notably reduced. Meanwhile, the DFT-parameterized kMC approach was also used to study hydrogen transport in the Fe-Cr binary alloys. The saddle-point energies for the TS-TS and TS-OS-TS pathways in both pure Fe and pure Cr were determined [64].

Also, based on DFT calculations, it has been noted that hydrogen can be easily trapped by the interface between carbide precipitates and the Fe lattice with possible hydride formation [60]. As the interstitial spaces in perfect cementite or carbides are small, hydrogen solubility and diffusivity in those lattices are very low. The coherent ferrite-cementite phase boundary is highly like to trap more hydrogen atoms compared to the ferrite or the cementite lattice [69]. Vacancies within the carbide and at the interface could serve as deeper trap sites with higher trap energy [70]. Recently, DFT calculations were conducted to investigate a series of carbide or nitride precipitates in α-Fe. The comparison between the defect free precipitates and vacancy-containing precipitates confirmed that the precipitate with a perfect lattice would not trap hydrogen while the vacancies reduce the hydrogen solution energy [71]. Due to the mechanical property disparities (i.e., stiffness mismatch) between the precipitate (cluster) and the Fe lattice, mismatch stresses and strains are expected near the interfaces which can enhance hydrogen trapping as well. In another study based on DFT calculations with transition state theory, vanadium carbide has shown good hydrogen permeability [72] as well.

By providing insights on the effects of hydrogen in heterogeneous materials, such computational approaches have the potential for enabling the discovery and design of suitable hydrogen barrier coatings.

3.2. DFT calculations for understanding hydrogen effects - extrinsic factors

In service conditions, such as in the case of transport of hydrogen in gas pipelines, the effects of hydrogen pressure and temperature should be considered as the hydrogen dissociative adsorption process, which is determined by the temperature and hydrogen partial pressure. DFT calculations have been performed to identify the hydrogen surface adsorption energy: the dissociative adsorption of hydrogen gas could happen on Fe (100) surface when the temperature is below 550 K and pressure ranges from 0.1 to 1.3 MPa. Increased hydrogen gas partial pressure and elevated temperature favor the dissociative adsorption of

hydrogen [73,74]. Meanwhile, the strain induced in the transportation system assemblies due to mechanical stress or thermal stress would also strain the interfaces and potentially enlarge the interstitial spaces which could increase hydrogen solubility as well.

The results of DFT calculations have been compared to experimental results. For example, both the hydrogen diffusivity in α-Fe [51] and aluminum [75], and the hydrogen solubility in different stainless steels and high entropy alloys [66] have been validated. DFT calculations have also been built to illustrate the grain boundary decohesion and embrittlement observed using APT [47]. Fe-Ti_2CS interfaces were also created to illustrate the different hydrogen solution energy in the Ti_2CS phase with different lattice structures [48].

The DFT calculations are computationally expensive and complex, especially for the metal atoms, such as Fe or Ni. Hence, most of the DFT-based investigations have been based on tens of supercells or a few hundred atoms in the models. If the magnetic properties of the atoms such as the proton's quantum fluctuations, lattice inharmonic vibrations, etc., are also considered in the DFT calculation, a more accurate predication could be obtained [51], while the computational cost is also significantly increased.

In recent years, the use of machine learning approaches with DFT calculations have generated machine-learning-based interatomic potentials or neural network interatomic potentials which can increase the accuracy of MD simulations to study hydrogen effects [76]. The ab initio MD (AIMD or first principles molecular dynamics) enlarges the sampling area for computing potential energy and enables MD simulations to produce results which are similar to those obtained with DFT calculations. AIMD has enabled an improvement in the cell sizes (atom numbers) and the computing time [63]. In summary, the DFT calculation is an important approach that provides valuable insights on the effects of hydrogen on a material due to intrinsic factors such as microstructural features and extrinsic factors such as temperature and pressure.

Details of the MD simulations approach for studying hydrogen effects on materials are discussed in the following section.

4. Molecular dynamics simulations for studying hydrogen effects

Compared to the DFT calculations, over billion-atom models have been simulated using the MD method [34,35], and the model size in one dimension can be over 100 nm. The large model size allows for the observation of the dislocation activity during plastic deformation and interaction of dislocations with hydrogen as well as other intrinsic features, such as precipitates, interfaces, and grain boundaries. Also, a longer simulation time period can be realized compared to the DFT calculations in the MD simulations and both tensile and shear stress could be applied to the model.

The MD simulations need the interaction potential functions or force fields to define the interaction between atoms. The potentials for the interaction of hydrogen with Fe [77,78], Fe-Cr [79], Al [80], Al-Cu [81], etc., have been developed and implemented as the embedded-atom method (EAM) or the modified embedded-atom method (MEAM) potential. Since the development of potential functions also cost great efforts, many MD simulations are conducted based on pre-developed potentials. Nevertheless, it is important to check different potential functions before being used in the MD simulations. Also, more than one potential is necessary if one single potential function could not cover all the elements present in the atomic structures that are analyzed. It is noted that some recent approaches have combined DFT and MD methods and invoked machine-learning approaches to develop interatomic potentials [82,83] and implemented these potentials in a moderate-size MD simulation as well [25].

4.1. MD simulations to understand fracture behavior

The "ductile to brittle transition" has been observed in the metallic materials tensile test after hydrogen charging, especially for the notched sample. The mechanism and the damage process associated with the embrittlement phenomena are generally difficult to capture in either DFT calculations or the continuum scale model. MD simulations using a longer simulation time and a larger model size can capture the effects of hydrogen which are not possible using the DFT calculations, which enhances the capability of investigating multiple intrinsic or extrinsic effects in one MD model, as illustrated in Fig. 4 (a). Models with different concentrations and distributions of hydrogen could be constructed by direct insertion into the matrix using the Monte Carlo method or can be realized by allowing for free diffusion at a high temperature in MD simulations. However, DFT calculations for hydrogen diffusion would typically need much longer computing times. During plastic deformation, hydrogen tends to diffuse from the perfect lattice sites to the lower-energy locations, such as the free surface on the cracks, crack tips, and the tensile-stressed region near newly formed dislocations. In the tensile or shear stretching process of a model with cracks, the crack expands and multiple crack branches are formed at the initial crack tip and new dislocations are also generated in the crack propagation process. These dynamic processes need sufficient model sizes to predict the crack propagation direction, which are often beyond the size of a typical DFT calculation.

Song and Curtin [86] built a 50 nm × 50 nm size model and adopted a modified Finnis-Sinclair type EAM potential for the Fe-H system. The effects of hydrogen concentration, loading rates, hydrogen diffusion, and crack/grain orientation were characterized in their MD model and in their analytical model. The MD simulation demonstrated that the ductile-to-brittle transition in steel was mainly caused by the suppression of dislocation emission at the crack tip because of a high hydrogen concentration. Higher hydrogen concentrations could change the HELP mechanism to hydrogen induced plastic zone compression [87]. Also, the effects of cyclical loads on the crack propagation were studied in steels and aluminum alloys [84,88]. The ductile-to-brittle transition is related to both hydrogen concentration and the pressure fluctuations generated by the loading spectra, as illustrated in Fig. 4 (b).

As the simulation times in the MD approach are much shorter compared to the time-scales over which experimental results are obtained, it is challenging to study the actual hydrogen adsorption and diffusion processes. Combined with a time-stamped force-bias Monte Carlo, the simulation time can be increased . In these long-time simulations, hydrogen is found to be concentrated near the cracked surface and to suppress fracture. It is found that the hydrogen atoms accelerate dislocation emission, enhance the generation of new dislocations, and increase dislocation mobility. As the model shown in Fig. 4 (c) [85], the hydrogen atoms accumulate in the active slip systems, and lead to the localization and planarity of the shear slip.

The effects of hydrogen on the motion of dislocations are quite subtle, especially during the crack propagation process. On the one hand, hydrogen is observed to promote dislocation movement which leads to the accumulation of dislocations at the crack tip which enhances plasticity at the crack tip. On the other hand, hydrogen is also observed to inhibit dislocation emission at the crack tip which makes it easy for the crack to expand and thus promotes brittle fracture. Both these hydrogen effects are reported in the MD simulations. The MD model and simulation conditions such as the potential functions, model setup, simulation settings, etc., adopted in the simulations can influence which of these two effects (i.e., increasing or decreasing localized plasticity) is observed more prominently in the actual simulations.

4.2. MD simulations to understand hydrogen-dislocation interactions

Besides the crack propagation simulation, the interactions between hydrogen and dislocations have been extensively studied to understand

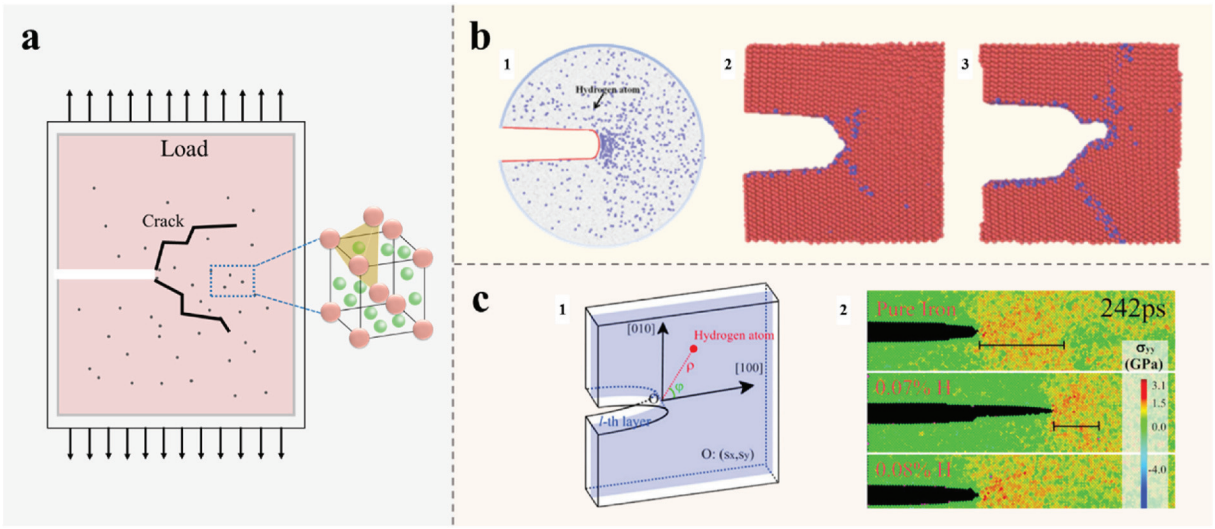

Fig. 4. MD simulations to understand fracture behavior: (a) the illustration of fracture model with hydrogen; (b) the effects of hydrogen concentration on the fracture behavior: (b.1) atoms distribution near the crack tips, (b.2) the ductile fracture and (b.3) brittle fracture [84]; and (c) the effects of hydrogen concentration on the stress near crack tips: (c.1) the hydrogen atom positions and (c.2) the comparison between models with and without hydrogen [85].

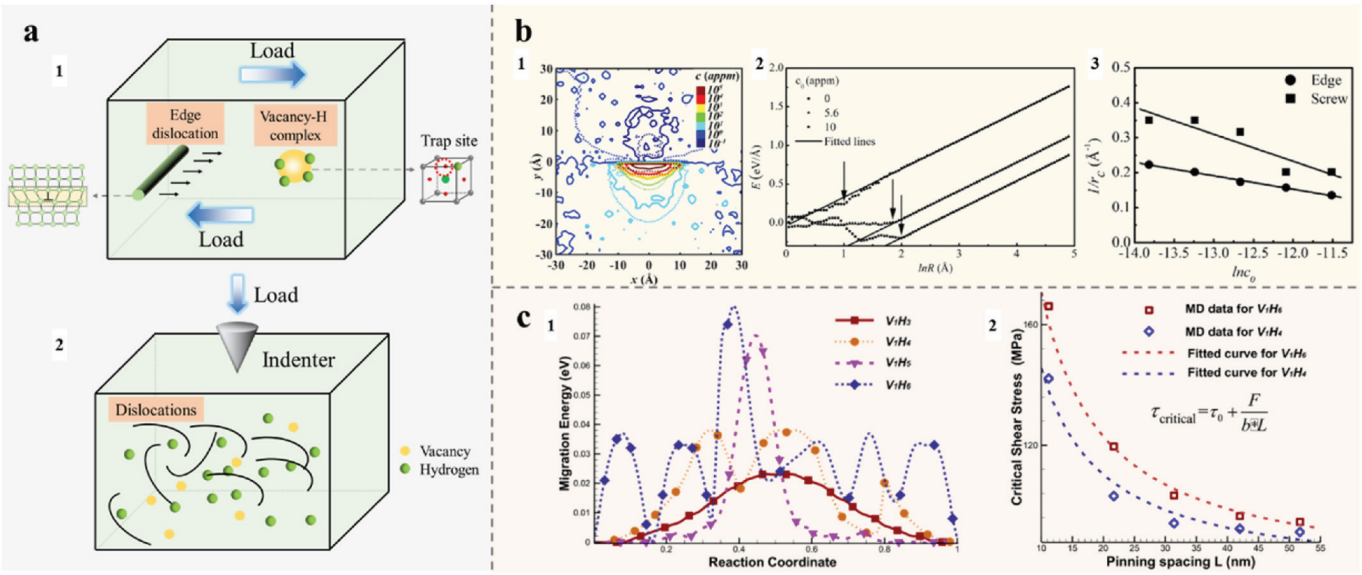

Fig. 5. MD simulations to understand hydrogen-dislocation interactions. (a) The illustration of hydrogen-dislocation interactions under (a.1) shear loads and (a.2) indentation; (b) the hydrogen-dislocation interactions: (b.1) the hydrogen concentration near the edge dislocation, (b.2) the effects of hydrogen concentration on the relationship between dislocation line energies and logarithmic outer cut-off radius (R), and (b.3) the relationship between the dislocation core radius (r_c) and the hydrogen concentration (c_0) for edge and screw dislocations [89]; (c) the effects of hydrides on (c.1) the migration energy and (c.2) the correlation between critical shear stress and the pinning spacing (average distance between vacancy-H complexes, L) [91].

the role of hydrogen in influencing plastic deformation in metallic materials, as illustrated in Fig. 5 (a.1). The "shielding effect" starts to influence the plastic deformation with hydrogen concentrations over 160 ppm. In the static state, the hydrogen distribution, stress, and the energy distribution near the dislocation have been studied. Using a modified EAM potential for the Fe-H system which represents the 12 shell binding sites within the Fe lattice, it was found that hydrogen has limited impact on the shear modulus and the stress field of the edge or screw dislocation. Most of the hydrogen atoms, which are located in the dislocation cores, reduce the dislocation energy and facilitate the dislocation movement, as shown in Fig. 5 (b) [89]. In a more complex Fe-C system which includes a ferrite-martensite (BCT structure with Fe_3C) dual phase structure [90], the added dislocations are found to reduce the hydrogen insertion energy in both phases, so more hydrogen could be trapped near the dislocations. Furthermore, more hydrogen atoms are found to be trapped in the martensite phase because of a high dislocation density and the carbon-included BCT structure.

Also, MD simulations have been invoked to investigate dislocation movement under shear stress [91,92]. The effects of hydrogen on the interaction between a moving dislocation and vacancies or vacancy clusters have been studied based on a simplified model, where the vacancy-H complex was utilized, as illustrated in Fig. 5 (a.1). It is found that the vacancy-H complexes have pinning effects on a moving edge dislocation, and the vacancy with more trapped hydrogen atoms exerting a higher pinning strength. On the other hand, the vacancy-H complexes with more hydrogen atoms also lead to a higher migration energy, as shown in Fig. 5 (c.1). These vacancy-H complexes could easily be converted to nano-voids after certain dislocation movement and thus

enable hydrogen embrittlement. It is noted that both the pinning spacing (distance between multiple vacancy-H complexes), as shown in Fig. 5 (c.2), and the shear rate would affect the critical shear stress obtained in the MD simulation. Therefore, the loading rate in the actual experiments is also expected to play a critical role in this embrittlement process.

The MD method has also been used to simulate nanoindentation and characterize the dislocation-hydrogen interactions through changes in the indentation loading curve, as illustrated in Fig. 5 (a.2) [93–95]. Under a rigid indenter, multiple dislocations are generated, so the effects between the hydrogen and dislocations can be observed clearly. In the FCC metal system, the loads corresponding to the onset of pop-in are reduced in a hydrogen charged sample. This is attributed to the shielding effect of dislocations by hydrogen, which reduces the barrier for dislocation nucleation. Also, the hydrogen was observed to decrease dislocation pile-up and enhance the movement of dislocations to the surface of the structure during the indentation simulations. It is also observed that the vacancies within the atomic structure have a more significant impact on the indentation loading curve than hydrogen [95]. More insights on the interactions between internal defects or interfaces with hydrogen during indentation are expected in future studies.

4.3. MD simulations to understand hydrogen-dislocation-grain boundaries interactions: bi-crystal models

DFT calculations and MD simulation have been combined to explore the energies of grain boundaries with a wide range of misorientation angles under different hydrogen pressures in thermodynamic equilibrium condition. The two methods were combined so that a system with a large number of atoms could be investigated and all the hydrogen trapping sites could be mapped. The energy analyses showed that the surface energy of the <100> symmetric tilt grain boundary is much lower than that of the free surface. However, the grain boundary region is more likely to trap hydrogen and the cohesive energy of the grain boundary is reduced by 37% because of the trapped hydrogen atoms. These simulations also indicate that the hydrogen trapping sites are unlikely to be fully occupied under low hydrogen pressures. Thus, hydrogen (or deuterium) would not be detected all along the grain boundaries [44]. Though the actual grain boundaries generally include more interstitial atoms, substitutional solutes, and high dislocation densities, the energy study indicates that the reduction in cohesive energy of the grain boundary leads to intergranular failure [96]. Therefore, controlling the grain boundary angles could help reduce the hydrogen trapping sites and thus minimize the reduction in the cohesive energy of the grain boundary, thereby, reducing the propensity for brittle fracture.

Bi-crystal models with a grain/grain boundary/grain structure have been developed to investigate the effects of the grain boundaries, as shown in Fig. 6 (a-c) [97,98]. As experimental observations using EBSD [99,100] indicate that most grain boundaries are symmetric tilt grain boundaries, the reported atomic models have been built based on such boundaries. For the Fe-H system with a certain concentration of hydrogen, the hydrogen concertation is shown to affect the yield strength of the bi-crystal system with both <100> and <110> symmetric tilt grain boundaries [55,101]. The hydrogen atoms enhance the dislocation movement and multiplication process and hence, the yield strength is reduced by ~30% in the bi-crystals models. Furthermore, the misorientation angle also affects the yield strength difference between the atomic structures with and without hydrogen and the hydrogen effects are also quite different for a given twist grain boundary [102].

The MD models with the interfacial screw dislocation network, where the dislocation density is correlated to the twist angles, also consist of solute hydrogen, grain boundaries, and screw dislocations, which are closer to the actual microstructures. The solute hydrogen would increase the tensile strength or the peak strength if the deformation mechanism is dominated by dislocation glide and the HELP mechanism is observed. However, the solute hydrogen would decrease the tensile strength if the deformation mechanism of the system is dominated by twinning and the deformation twins grow faster in those models. Also, the vacancies were not notably increased in the model with the solute hydrogen and the twinning dominated deformation. The twinning deformation would help reduce the effects of solute hydrogen in certain regions.

Besides simulations of tensile deformation, simulations of shear deformation were also conducted on the bi-crystal system where two grains were rotated around the [1$\bar{1}$0] tilt axis to different degrees to construct different grain boundaries [98,101]. Compared to the atomic simulation under tensile loads, it is difficult to observe debonding or

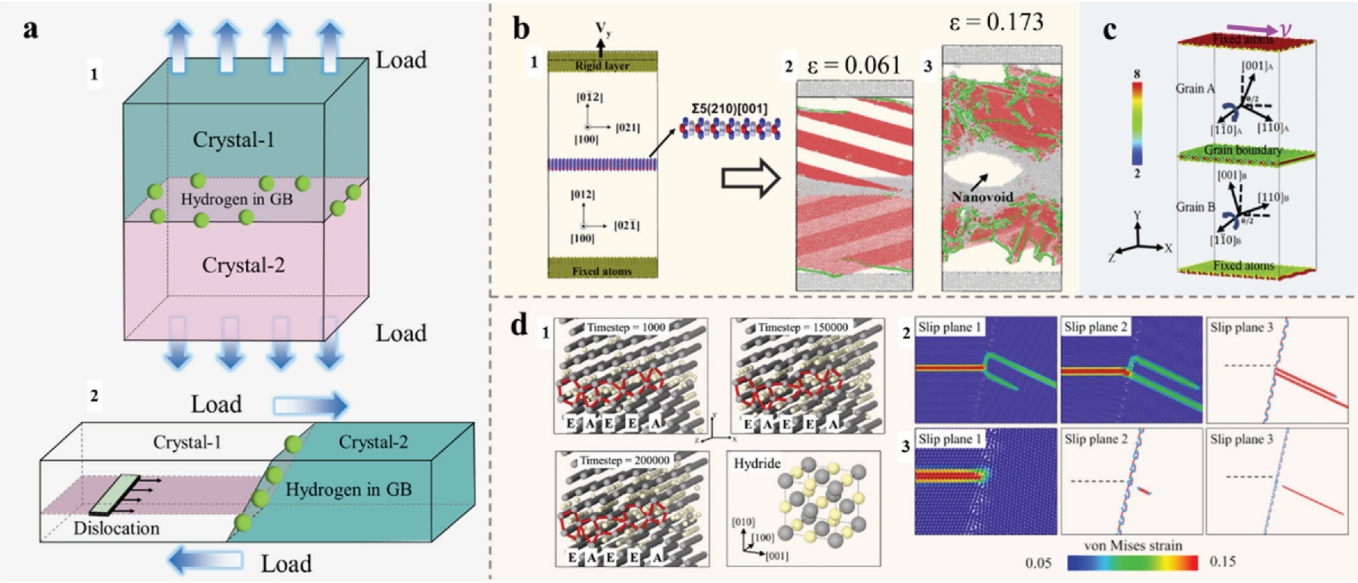

Fig. 6. MD simulations to understand hydrogen-dislocation-grain boundaries interactions. (a) Illustration of bi-crystal model under (a.1) tension and (a.2) shear loads; (b) bi-crystal model with Σ5 grain boundary: (b.1) the modeling setup, (b.2) the model with strain at 0.061 and (b.3) nanovoids formation with strain at 0.173 [97]; (c) the setup for bi-crystal modeling with <110> grain boundaries under shear loads [98]; and (d) the effects H segregation on the grain boundary: (d.1) hydride formation at the Σ27 (552) grain boundary in Ni lattice, and the strain value obtained for the interaction between (d.2) the screw dislocation and H-free and (d.3) the screw dislocation and H-segregated Σ179 (779) grain boundary [103].

total separation between atoms in the atomic-scale shear modeling. Hence, the shear stress rather than strain is generally adopted to numerically illustrate the hydrogen effects. It is observed that different types of grain boundaries show different hydrogen effects in the shearing deformation mode. The shear stress of the system with Σ9 grain boundary was significantly increased, while the shear stress was almost the same in the model with Σ19 grain boundary. In the tensile deformation case, it is difficult for the grain boundary to migrate, while in the shear deformation case, grain boundary migration is readily observed. Such migration suppresses hydrogens cluster growth and prevents brittle failure due to the formation of hydrogen voids.

The interactions between screw dislocations and nine types symmetric tilt grain boundaries (with misorientation angles from 20° to 180°) were studied by using MD simulation with or without hydrogen atoms [104]. Based on the shear stress-strain curves, four stages of interactions, i.e., dislocation dissociation, transmission, nucleation, and reflection were observed for the general dislocation-grain boundary interaction without hydrogen. In general, hydrogen converted the dislocation dissociation step to the dislocation absorption step, except in the case of twin grain boundaries which do not trap many hydrogen atoms. The impediment effects of hydrogen bring a new interaction mechanism between dislocation and grain boundaries. The low-energy grain boundaries (such as the twin boundaries) could be an effective barrier for dislocation interaction.

Interactions between screw or 60° dislocation and 18 [1$\bar{1}$0] symmetric tilt grain boundaries were also studied, as shown in Fig. 6 (d) [103]. The simulation showed that hydrogen atoms trapped at the grain boundaries mainly change the lattice dislocation-grain boundary interaction. The formation of hydrides near the grain boundary would prevent the dislocation gliding on the grain boundary and dislocation nucleation and emission near the grain boundary becomes difficult.

Also, a more complex model was established to study the effects of hydrogen in a α-Fe atomic structure with dislocations and Σ3 <110> (112) symmetric tilt grain boundaries [105]. Under tensile deformation, the solute hydrogen atoms exhibit pinning effects and decrease the velocity of the edge dislocations. So, the hardening in the stress-strain curve was observed with pre-existing dislocations. Hydrogen also increased the energy for the dislocation to go across the grain boundaries, so segregation was observed near the grain boundary.

The bi-crystal model was further utilized to explore fracture under tensile loading conditions. A new bi-crystal model was constructed with the following geometry - grain boundary-2/grain/grain boundary-1/grain/grain boundary-2, so that two complete grains could be investigated [106]. It was found that the stress-strain curves of the models with Σ31 grain boundary were not affected by the hydrogen concentration. Meanwhile, the stress of the models with Σ9 grain boundary was reduced with hydrogen and a higher hydrogen concentration leads to a higher stress reduction. After high strain deformation, dislocation impingement and emission near or at the grain boundary is "activated" and cause nanovoid nucleation and growth. With a high hydrogen concertation (or more solute hydrogen), voids nucleation and coalescence, or even, cracks near the grain boundaries were observed. Thus, the grain boundary type and misorientation angles within a microstructure could serve as a clue to determine suitability of the material in a given service environment and the safe loads for operation. It was also noted that the differences between the stress-displacement obtained from the Fe-H EAM, which is widely implemented [107], and DFT calculation is quite significant if the distance between atoms exceeds 2 Å. Thus, a carefully calibrated potential function would be needed for MD simulations.

Besides the recent progress in steels, bi-crystal models were also invoked to study the hydrogen effects in FCC Ni. It was found that hydrogen has a significant impact on the grain boundary, such as the Σ3 <110> twin grain boundaries [108]: the hydrogen concertation affects the segregation near the inclined twin grain boundaries and the higher hydrogen concentration could bring in the defaceting transition to the grain boundary.

In the bi-crystal model without crack tips, over 10 types of grain boundaries were studied and the hydrogen concentration, 0.1 hydrogen atom per Å^2, showed embrittlement in the atomic structure under tensile load [109]. When the hydrogen diffusion process was coupled with deformation, the maximum reduction of tensile strength and fracture energy reached 6.60% and 15.75% for atomic models with Σ5 (210) <100> and Σ17 (530) <100> grain boundaries, respectively. In these MD simulations, grain boundaries were represented by several layers of highly distorted atoms. These highly distorted atoms brought in boundary disruption effects which resulted in the atoms in this region are not always under tensile stress during deformation. Hydrogen accelerated embrittlement with these two effects.

The energy of the grain boundaries was also studied in the bi-crystal model. With 0.01 at.% hydrogen in the structure, the atomic models with low energy grain boundaries (grain boundary energy <10 mJ/m^2) and high energy grain boundaries (grain boundary energy >1200 mJ/m^2) were constructed [110]. Hydrogen changed the strength of the atomic system with low and high energy grain boundaries by +4% and −15%, respectively. The grain boundary types as well as the grain boundary energy are noted to be the dominant factors in determining the coupling effects of hydrogen, dislocations, and grain boundaries under tensile deformation. Hydrogen also induces instability to high energy grain boundaries, such as Σ9 (221) or Σ27 (115) grain boundary, by enhancing dislocation nucleation and emission while suppressing the low energy grain boundaries, such as Σ1 (001) or Σ3 (111) grain boundary. If grain boundary energy is accurately computed at room temperature instead of 0 K, and the effects of certain non-equilibrium processing conditions are considered, then the correlation between grain boundary energy, misorientation angles, and hydrogen would be more meaningful to guide grain boundary engineering for hydrogen embrittlement resistance.

A specific hydrogen-controlled plasticity mechanism was also proposed based on an bi-crystal model with a Σ5 (210) [001] grain boundary, which traps more hydrogen atoms than the Σ3 coherent twin boundary [111]. In the canonical Monte Carlo and MD combined model, different hydrogen concentrations and their effects in changing the fracture process from transgranular to intergranular fracture were studied. It was found that the hydrogen atoms in the structure suppress the stress-releasing ability of the grain boundary so that a build-up of the local stress concentration takes place. Local plastic deformation near and at the grain boundary leads to dislocation emission, severe twinning evolution, and more vacancies. Subsequently, the vacancies grow and nanovoids are formed at the grain boundary. The size of the nanovoids increased with hydrogen which enabled the transition of fracture mode from transgranular to intergranular fracture.

Also, the bi-crystal atomic model was further modified by adding a crack tip to study the intergranular fracture of Ni. The grain boundaries with Σ3 misorientations were further investigated in the MD model which included a crack at the center of the bi-crystal model [112]. The concept of atomistic cohesive zone volume elements (observation windows for monitoring crack propagation) was introduced and tensile deformation was simulated to obtain the traction-separation relationship. It was found that the crack tip would extend faster with a higher hydrogen concentration in the model. The peak stress of the atomic system is also reduced with a higher hydrogen concentration. Additionally, double cracks were introduced in the bi-crystal models to simulate the effects of the segregation of hydrogen at/near the grain boundaries on the crack tip extension behavior. The MD simulations covered Σ3, Σ9, and Σ99 type grain boundaries, and the obtained simulated values were used to calculate the critical stress intensity factor with Griffith and Rice theory. The comparison between MD models with and without hydrogen indicates that hydrogen facilitates the brittle crack growth or accelerates the intergranular fracture in the brittle fracture case. Meanwhile, it is quite interesting to see that the twin

boundaries do not absorb hydrogen in the fracture process. Thus, Ni based engineering material with a larger percentage of twin boundaries could potentially lower the possibility of hydrogen embrittlement.

The interaction between crack tips and hydrogen is rather complicated because both the accuracy of the EAM and the way of creating cracks in the model impact the model results. Another study focused on the interactions between the crack tips and hydrogen/hydride considering the effect of hydrogen diffusion near the crack tip and along the crack propagation path in a single crack model [113]. By including four types of hydrogen mapping conditions, such as (1) no hydrogen atoms along the grain boundary, (2) hydrogen atoms fully occupying all the grain boundary trapping sites, (3) hydrogen atoms occupying all the grain boundary trapping sites and having the option to migrate from the trapping sites to the surface, and (4) all surfaces are occupied with hydrogen atoms, it was found that embrittlement was likely to happen in the bi-crystal model only with assumption (4). In the model with Σ19 type grain boundary, embrittlement would not happen under the other three assumptions. Therefore, the use of a more accurate hydrogen mapping approach in the non-equilibrium dynamic process would be a crucial step for studying hydrogen embrittlement.

With a similar single crack bi-crystal model, the effects of hydrogen as well as temperature (77 K–600 K) on the fracture mode, were explored [97]. The Σ5 (210) [001] symmetric tilt and Σ9 $(1\bar{1}0)$ $[22\bar{1}]$ pure twist grain boundaries were studied as both boundaries are the low-angle ones. Temperature effects were observed to be quite subtle: at low temperatures hydrogen-promoted intergranular fracture was observed which has been demonstrated by both the atomic simulations and experiments [114]; at high temperatures vacancy formation is facilitated at low hydrogen concentration while the vacancy-hydrogen complexes are destabilized if the hydrogen concentration is high [115]. Temperature has different effects on nucleation of dislocations and the hydrogen-dislocation interaction is not the main factor that results in the final intergranular fracture. The critical hydrogen concentration concept, which could be deduced based on the temperature, hydrogen concentration, vacancy distribution, and local strain was proposed to predict the complete intergranular fracture behavior. Also, this concept could be utilized to estimate critical hydrogen concentration or even the service time for materials if the diffusion model was combined with the specific microstructure (grain boundary type and fraction), temperature, and loading.

4.4. MD simulations to understand hydrogen-polycrystalline structure interactions

In addition to bi-crystal models, polycrystal models have also been recently developed for Al [116], Fe [117–119], and Ni [120], as illustrated in Fig. 7 (a). In the 2D nanograin-sized atomic Fe models, as shown in Fig. 7 (b), the grain size ranged from 5 nm to 24 nm with the same microstructural features, such as grain arrangement and orientation. For the model with a grain size of 10 nm, the uniaxial tensile stress of the model reaches the maximum value. Because of the hydrogen effects, the normally expected inverse Hall-Petch relation was converted to the normal Hall-Petch relation when the grain size is less than 10 nm: the small grain size models (with grain size less than 10 nm) would have more trapped hydrogen at the grain boundaries and are more likely to go through an intergranular deformation; while the large size model (with grain size greater than 10 nm) would involve more hydrogen effects on the dislocation-hydrogen interaction, but those influences are small. Also, under different temperatures and stress, the dominant deformation mechanism, i.e., the creep behavior of polycrystal Fe, was found to be affected by the hydrogen interaction with microstructural features as well.

In 3D models of polycrystalline aluminum, where an actual hydrogen concentration that is typically present in cast aluminum alloys (i.e., 0.001 at. %) was used, it was found that this low concentration of hydrogen did not affect the tensile strength of the aluminum alloys. However, the hydrogen accumulation near the interfaces or grain boundaries could lead to the creation of internal defects and affect the ductility of aluminum alloys. 3D polycrystalline atomic models were also created for Ni alloys with 7.5 nm grain size as shown in Fig. 7 (c). A strain of 10% was imposed on the model and a dislocation network was generated. It was found that hydrogen atoms preferred to stay at the grain boundaries rather than dislocations and these hydrogen atoms did not have any obvious pinning effects on the dislocation motion. Hydrogen did not affect the von Mises stress distributions in the 3D model as almost similar results were obtained for simulations with and without hydrogen [120].

There have been fewer studies that have used MD simulations for

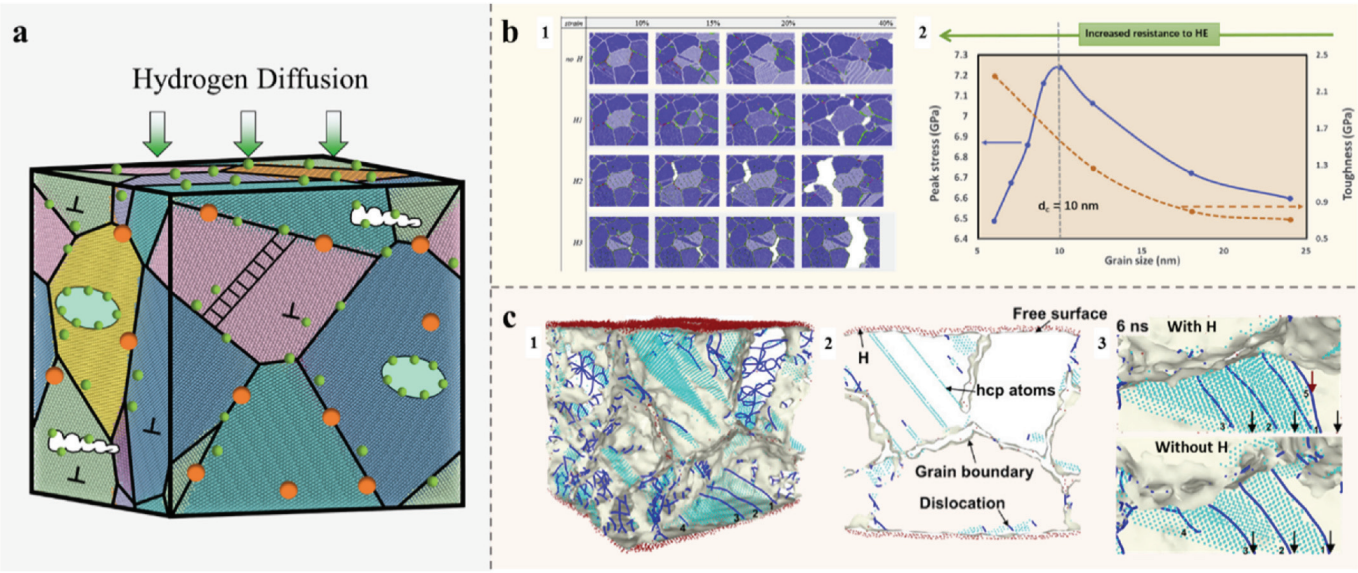

Fig. 7. MD simulations to understand hydrogen-polycrystalline structure interactions. (a) The illustration of polycrystalline models in MD simulations; (b) the effects of hydrogen on the deformation of nanograin-sized Fe: (b.1) the tensile deformation of the model with 12 nm sized grain, and (b.2) the relationship between peak tensile strength/toughness and grain size [117]; and (c) the effects of hydrogen on the deformation of nanograin sized Ni: (c.1) 3D model, (c.2) 2D view for modeling setup, and (c.3) dislocation rearrangements after 6 ns time [120].

stainless steels as multiple atom interaction potentials were not readily available. Zhou et al. developed Fe-Ni-Cr-H EAM potential [121] and investigated the stacking fault energy with hydrogen in the Fe-Ni-Cr austenitic stainless steels using MD simulation [122]. Three alloy systems: $Fe_{0.70}Ni_{0.11}Cr_{0.19}$, $Fe_{0.70}Ni_{0.1}Cr_{0.2}$, and $Fe_{0.70}Ni_{0.15}Cr_{0.15}$ were investigated. They found that hydrogen atoms reduced the average stacking fault energy of stainless steel and a higher hydrogen concentration at the dislocation core intensified the influence of hydrogen on the stacking fault energy.

In these MD simulations, the accuracy of the simulation results may be less than that obtained in the DFT calculation since the empirical potential functions were utilized. However, the mechanisms of dislocation-grain boundary-hydrogen interaction were well studied in MD simulations and the hydrogen effects on the plastic deformation processes were well elucidated.

5. Continuum scale modeling for studying hydrogen effects

At the continuum scale, the finite element method (FEM), the phase field method (PFM), and discrete dislocation dynamics (DDD) have been utilized to analyze dislocation motion, hydrogen trapping and diffusion, and hydrogen-related non-linear fracture processes within the materials. The continuum scale simulated results can be directly validated with experimental results as the time and length scales are similar. However, the hydrogen effects on the intrinsic microstructural features, which have been discussed in the previous section, should be carefully introduced in the continuum scale models, as illustrated in Fig. 8.

Hydrogen diffusion in metallic materials was investigated through the finite element method on a much large scale compared to the atomistic models discussed in the previous section. Based on a mechanical-diffusion coupled model, stress-assisted diffusion and trapping because of the plastic strain were studied [129]. Various properties such as grain size, grain orientation, the elastoplastic properties of α-Fe, and trap density related to dislocations and external factors such as temperature and hydrogen pressure were linked. No obvious inhomogeneity in the hydrogen concentration was observed in the polycrystalline bulk material. The hydrogen transport in the polycrystalline structure was found to be twice as much slower than transport in a single crystalline structure with no grain boundaries. Besides pure iron, steels are generally manufactured with carbides or inclusions in them and thus more hydrogen trapping sites could be introduced in steels because of vacancies within these carbides and the incoherent interface. The finite element method-based diffusion model was proposed based on three Fe-C-Ti materials to simulate the hydrogen trapping and diffusion in a 1 mm thick steel sample [130]. The constitutive model, with the thermal desorption spectra results, was able to calculate trap density and binding energy under a certain hydrogen flux and temperature. The trapping energies for the steels ranged from 58 kJ/mol (0.61 eV) to 110 kJ/mol (1.14 eV). Also, the hydrogen traps were strongly correlated to the carbon vacancies in TiC precipitates. Furthermore, the effects of the phase boundaries on the hydrogen diffusion, such as ferrite-austenite interfaces in dual phase steels, were studied based on a mass diffusion model considering different solubility cases [123]. Hydrogen needs certain energy to move across the ferrite-austenite phase boundary, and this energy barrier was considered in the study, as illustrated in Fig. 8 (a.1). With the actual microstructure, hydrogen diffusion within the dual-phase microstructure at long times (i.e., 16 h) and high temperature (i.e., 600 K) were predicted. It was found that the presence of austenite as well as its morphology (the elongated austenite grains aligned normally to the diffusion direction) reduces the steady-state

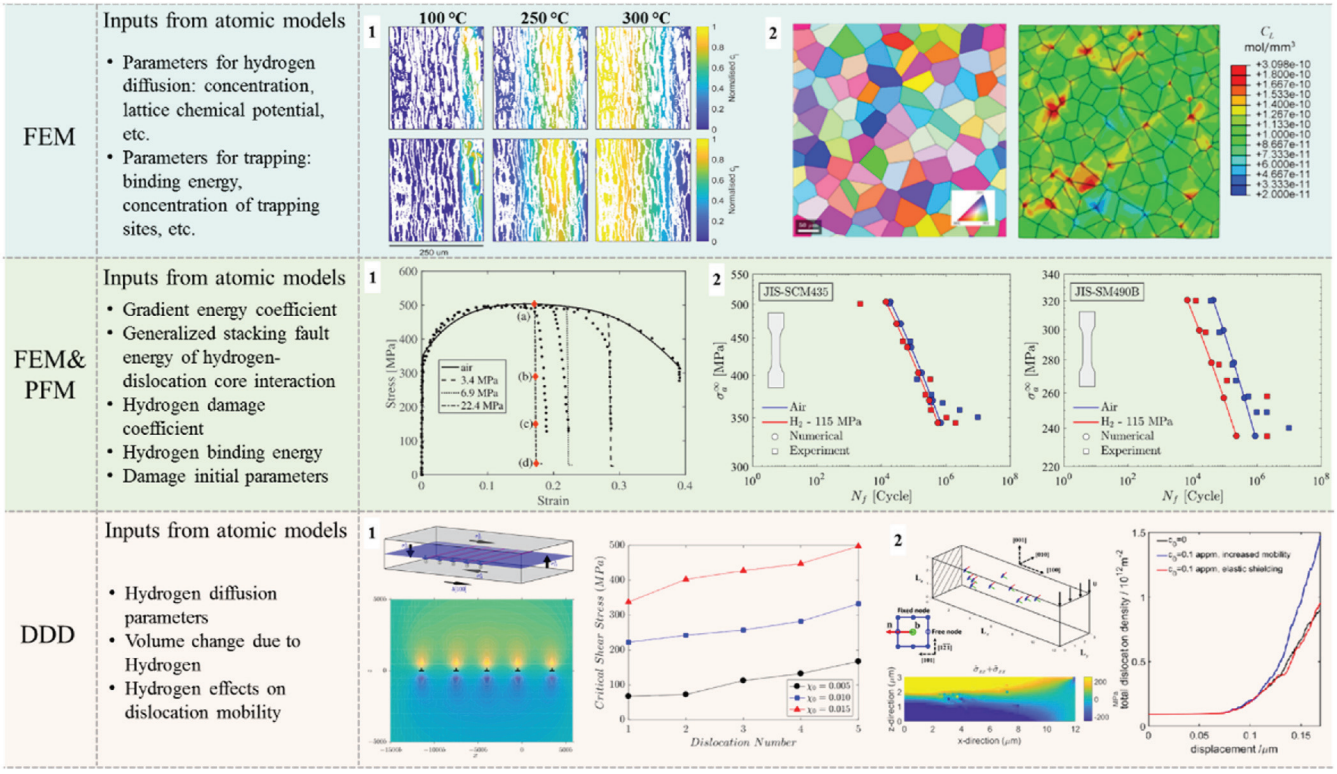

Fig. 8. The continuum scale models for studying hydrogen effects. (a) Finite element method (FEM): (a.1) the normalized hydrogen concentration in the austenite phase under different temperatures [123], and (a.2) the hydrogen concentration prediction based on the representative volume element (RVE) approach [124]; (b) coupled finite element method and phase field method (FEM&PFM): (b.1) a coupled diffusion-deformation-damage model approach for stress-strain curve prediction [125], and (b.2) numerical predicted and experimental measured S-N curves for two steels under 115 MPa hydrogen pressure [126]; and (c) The discrete dislocation dynamic (DDD) method: (c.1) the model setup to investigate the effects of hydrogen on the critical shear stress and dislocation numbers [127], and (c.2) a cantilever model to study the effects of hydrogen on dislocation density [128].

hydrogen flux and the effective diffusivity. Besides the actual microstructure based modeling, the representative volume element (RVE) approach has also been utilized to illustrate the effects of external loads on the trapping sites as well as the hydrogen diffusion, as illustrated in Fig. 8 (a.2) [124]. A diffusion coupled crystal plasticity model was developed so the effects of the inhomogeneous strain on the hydrogen accumulation at the grain boundaries could be numerically illustrated. It was found that under a high hydrogen pressure (such as over 100 bar), the hydrogen concentration in a high strength steel is dominated by the hydrogen trapped in the deformed lattice after 3% strain.

The hydrogen-assisted fracture or crack models in the continuum scale are rather complex as they have to consider the trapping and diffusion of hydrogen, hydrogen sensitivity properties, the fracture surface energy, the coupled unstable and non-linear crack growth, etc. [125,126,131–133]. A coupled mechanical-diffusion-phase field finite element framework has been proposed and the critical Griffith-type energy release rate, which is dependent on the hydrogen coverage and hydrogen damage coefficient,and the hydrogen-dependent surface energy calculated by the DFT method, has been implemented. Good correlation between the experiments and model prediction in: (1) section strength versus hydrogen concentration in the single notched bar for AISI 4135 steel; (2) section stress versus load time in single edge notched specimen for dual phase steels; and (3) stress intensity factor versus hydrogen concentration in compact tension specimens for AerMet100; were achieved. A sophisticated model that couples the diffusion of hydrogen with the elastic-viscoplastic material characteristics has been proposed by Anand et al. [125], where the concept of crazing was introduced and the strain produced by the crazing was treated as the quasi-brittle form of inelastic deformation. A good fit for the elongation of one ferritic steel under different hydrogen pressures (3.4-22.4 MPa) was achieved for the modeling prediction and experiments, as illustrated in Fig. 8 (b.1). Also, the actual microstructures were converted to micromechanical finite element models to predict the fatigue crack initiation lifetimes [132]. The crystal plasticity model and the hydrogen diffusion model were coupled and the combined model predicted the fatigue crack initiation time in a 1 MPa hydrogen pressure environment. Later, a deformation-diffusion-damage coupled model was developed to numerically evaluate the hydrogen effect on the fatigue crack nucleation and growth under cyclic loads based on the phase field fracture method [126]. The fatigue life (the S-N curve) of two steels (JIS-SCM435 and JIS-SCM490B) under a much higher hydrogen pressure, ~115 MPa, were predicted, as shown in Fig. 8 (b.2). Good correlation between experiments and simulation were achieved up to a million cycles of loading. Using experimentally observed fatigue crack growth rate behavior of pipeline steels under different hydrogen atmospheres, a master curve for the fatigue crack growth behavior has also been generated which can be used for fatigue life prediction in the presence of flaws in pipelines [134–137]. For these continuum models, there are many hydrogen-related parameters such as hydrogen solubility, hydrogen diffusion, hydrogen trapping at dislocations or grain boundaries, hydrogen-induced damage initiation and evolution, and the accurate calibration of these parameters is a challenging task.

Furthermore, large-scale, three-dimensional discrete dislocation dynamics simulations were conducted to investigate the interaction between hydrogen and dislocations at the meso-scale (such as in a 108 μm^3 bulk sample) [127,128,138], as shown in Fig. 8 (c). In these dislocation dynamics simulations, the parameters for hydrogen diffusion, the chemical potentials of hydrogen, the hydrogen-related dislocation mobility equations, etc., are needed as input. In the simulations for the bulk material without external stress, the shielding effect is observed for Ni which possesses a high hydrogen diffusion coefficient. The shielding effect leads to a decrease in dislocation separation distances for parallel edge dislocations. The hydrogen around the edge dislocations would have pinning effects in α-Fe which possesses a small hydrogen diffusion coefficient. So, higher stresses are needed to remove the pinning effects of the dislocations due to hydrogen. On the other hand, at the experimentally validated hydrogen concentrations, hydrogen is also observed to promote dislocation generation, enhance slip planarity, and reduce the screw dislocation percentage. These discrete dislocation dynamics simulations support the HELP mechanism [128].

In the continuum scale, the hydrogen-related parameters represent the interaction between hydrogen and the intrinsic nano-/micro-structural features which have been studied using the atomic scale calculations and simulation. Therefore, the "bottom-up" approach would be possible to predict the performances of given material under a hydrogen environment.

6. Discussions and outlooks for multi-scale modeling approaches

As shown in Fig. 9, the recent progress made in understanding hydrogen effects using multi-scale simulations can be summarized as follows: the atomistic calculations based on the DFT method provides the fundamental physical properties, such as hydrogen diffusion and trapping sites, and the data for interaction potentials for the MD based simulation; the MD based simulations are able to characterize the effects of the grain boundaries in a 100 nm size region; the dislocation dynamic simulations can model the interactions between the hydrogen and dislocations in a 10 μm region; and the continuum level models can include the effects of microstructure, cracks and the hydrogen-related parameters for strength, elongation, and fatigue life prediction. In recent years, more novel atomic-scale computational efforts, have been developed to include the actual nano-/micro-structural features and the results have been validated with experimental observations. Thus, the potential for developing multi-scale computational tools to predict the performance of metallic materials in hydrogen environments, especially for hydrogen transportation, has been well recognized [139–141].

However, multiple tasks need further investigation for more accurate predictions. Grain boundaries are generally assumed to be perfect and homogenized interlayers in the DFT calculations or MD simulations. However, as the experimental observations based on the APT [40,47,142] and nanoindentation [100,143,144] show, grain boundaries or incoherent interfaces should include both composition heterogeneity (such as the element segregation) and structure heterogeneity (such as the vacancies or defects). Therefore, the effects of the boundary require further investigation.

In the MD simulations, the accuracy of the simulation results would be less than that obtained from DFT calculations since empirical potentials are utilized. Although the newly developed machine-learning-based interatomic potentials could improve the accuracy of MD simulations, the computing time would be prolonged as well. Also, most of the MD simulations are conducted with the Fe-H or Fe-Fe EAM potentials while the actual steels contain more elements and different compositions. MD simulations of hydrogen effects with new interaction potential functions that include more elements (such as Si, Mn, Cr, Ni, etc.) in models with internal defects (such as vacancies) and subjected to strain and temperature, would transform MD simulations from a mechanism studying tool to a property prediction tool.

Metallic materials, such as dual phase steels and stainless steels, with austenite grains, can undergo martensitic transformation and the strength of the steel will be increased. For the metallic materials used for liquid hydrogen storage and transportation, hydrogen at low temperatures affects the phase transformation as well as the material's strength. Although there have been extensive experimental studies [145–147] and numerical simulations on materials without hydrogen effects [148], neither atomistic nor continuum scale numerical simulation of phase transformations with hydrogen effects have been reported. While the appearance of new phases can be discerned in MD simulations by noting the atomic positions after deformation [86], the martensitic transformation is quite complex to capture. Future work in this field will improve the understanding of the hydrogen effect on phase

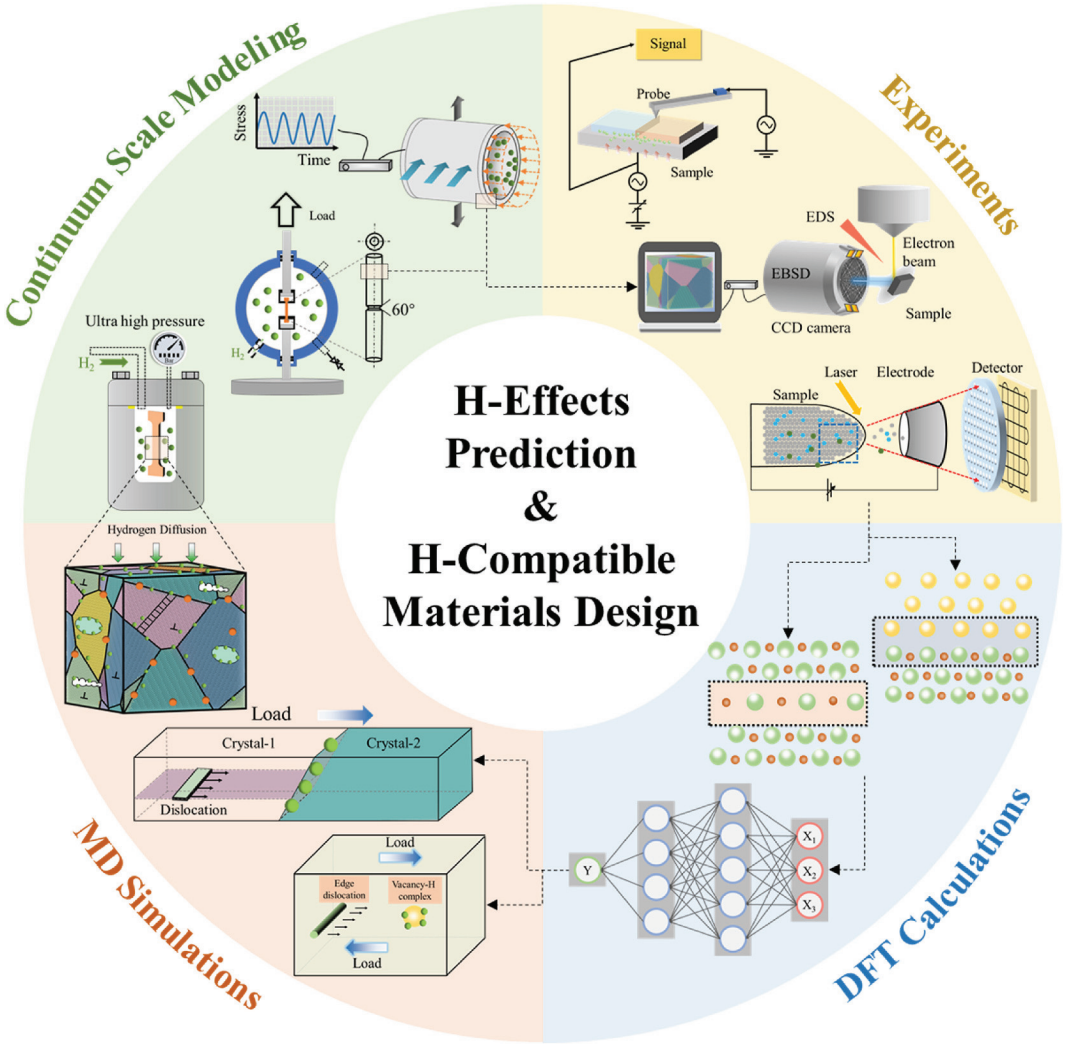

Fig. 9. The summary of the current review for hydrogen effects prediction and hydrogen compatible materials design. Experiments section includes PFM, APT and EBSD; DFT calculation section includes interfaces, boundaries and machine learning for EAM; MD simulations section includes hydrogen (vacancy complex) and dislocations interaction, hydrogen-dislocation-grain boundary interaction and hydrogen-polycrystalline; and continuum scale modeling section includes hydrogen diffusion in materials, and the effects of hydrogen on materials strength and fatigue life.

transformation and accelerate the design of hydrogen compatible materials.

The size effect is quite obvious in the multi-scale study with the strength obtained in the atomic simulations being much higher than the experimentally observed strength and being close to the theoretical tensile strength [33]. With a larger atomic model that can include defects and a longer simulation time, the strength obtained from the atomic simulation is expected to be reduced and become closer to the values observed in macroscopic experiments. Similarly, the elastic modulus obtained from the simulations should be similar across different length scales as well. The instrumented indentation method enables the determination of the elastic modulus using the indentation unloading curve (Oliver-Pharr method). Furthermore, the interaction of hydrogen with intrinsic factors, such as the vacancies [95], precipitates [149], and grain boundaries, can be assessed through the indentation loading curve. Besides the SKPFM, indentation or force probing-based experiments could be powerful tools to assess the effects of hydrogen on plastic deformation characteristics and bridge atomistic simulations with continuum modeling [143].

7. Summary

The successful realization of a hydrogen economy is crucially dependent on a comprehensive understanding of the effects of hydrogen on the hydrogen infrastructure materials and the development of hydrogen compatible materials with long term reliability. Progress made in recent times in understanding the fundamentals of hydrogen embrittlement mechanisms in metallic materials has been reviewed. Particular emphasis has been made on highlighting the challenges and breakthroughs made in the simulation of hydrogen effects across multiple length-scales using the DFT method, MD simulations and continuum approaches. The DFT approach is an important approach that provides valuable insights on the effects of hydrogen on a material due to intrinsic factors such as microstructural features and extrinsic factors such as temperature and pressure. MD simulations of hydrogen effects with new interaction potential functions that include more elements (such as Si, Mn, Cr, Ni, etc.) in models with internal defects (such as vacancies) and subjected to strain and temperature, could transform MD simulations from a mechanism studying tool to a property prediction tool. The continuum levels models have the potential to incorporate the effects of microstructural features and predict the mechanical performance of materials, such as deformation and fatigue life under hydrogen

environments. Overall, there is positive outlook for developing multi-scale computational tools for designing hydrogen compatible materials and for predicting the performance of metallic materials in hydrogen environments using a bottom-up approach.

Credit author statement

Guang Cheng: Conceptualization, draft, Writing – Original, Investigation, Writing - Review & Editing, Supervision, Funding acquisition; **Xiaoli Wang:** Writing – Original, draft, Investigation, Visualization; **Kaiyuan Chen:** Writing – Original, draft, Investigation, Visualization; **Yang Zhang:** Conceptualization, draft, Investigation, Visualization; **T. A. Venkatesh:** Conceptualization, Writing - Review & Editing, Investigation, Supervision, Funding acquisition; **Xiaolin Wang:** Conceptualization, Investigation, Supervision, Funding acquisition; **Zunzhao Li:** Supervision, Investigation, Funding acquisition; **Jing Yang:** Supervision, Investigation, Funding acquisition.

Declaration of competing interest

The authors declare that they have no known competing financial interests or personal relationships that could have appeared to influence the work reported in this paper.

Data availability

Data will be made available on request.

Acknowledgements

Guang Cheng acknowledges the support from the National Natural Science Foundation of China (51905026), and the Fundamental Research Funds for the Central Universities (buctrc201827). T. A. Venkatesh acknowledges the support from the National Science Foundation (DMREF grant #2119337). The authors (Guang Cheng, Xiaoli Wang, Kaiyuan Chen, Yang Zhang, Xiaolin Wang, Zunzhao Li, Jing Yang) acknowledge the support from the research project from Science and Technology Department of SINOPEC (322120).

References

[1] Johnson WH. On some remarkable changes produced in iron and steel by the action of hydrogen and acids. Nature 1875;11(281):393. https://doi.org/10.1038/011393a0. 393.
[2] Hirth JP, Rice JR. On the thermodynamics of adsorption at interfaces as it influences decohesion. Metall Trans A 1980;11(9):1501–11. https://doi.org/10.1007/BF02654514.
[3] Yamaguchi M, Kameda J, Ebihara K-I, Itakura M, Kaburaki H. Mobile effect of hydrogen on intergranular decohesion of iron: first-principles calculations. Philos Mag A 2012;92(11):1349–68. https://doi.org/10.1080/14786435.2011.645077.
[4] Koyama M, Tasan CC, Akiyama E, Tsuzaki K, Raabe D. Hydrogen-assisted decohesion and localized plasticity in dual-phase steel. Acta Mater 2014;70:174–87. https://doi.org/10.1016/j.actamat.2014.01.048.
[5] Martin ML, Dadfarnia M, Nagao A, Wang S, Sofronis P. Enumeration of the hydrogen-enhanced localized plasticity mechanism for hydrogen embrittlement in structural materials. Acta Mater 2019;165:734–50. https://doi.org/10.1016/j.actamat.2018.12.014.
[6] Djukic MB, Bakic GM, Sijacki Zeravcic V, Sedmak A, Rajicic B. The synergistic action and interplay of hydrogen embrittlement mechanisms in steels and iron: localized plasticity and decohesion. Eng Fract Mech 2019;216:106528. https://doi.org/10.1016/j.engfracmech.2019.106528.
[7] Nagumo M, Nakamura M, Takai K. Hydrogen thermal desorption relevant to delayed-fracture susceptibility of high-strength steels. Metall Mater Trans A 2001;32(2):339–47. https://doi.org/10.1007/s11661-001-0265-9.
[8] Sofronis P, Birnbaum HK. Mechanics of the hydrogen-dislocation-impurity interactions—I. Increasing shear modulus. J Mech Phys Solid 1995;43(1):49–90. https://doi.org/10.1016/0022-5096(94)00056-B.
[9] Birnbaum HK, Sofronis P. Hydrogen-enhanced localized plasticity—a mechanism for hydrogen-related fracture. Mater Sci Eng, A 1994;176(1):191–202. https://doi.org/10.1016/0921-5093(94)90975-X.
[10] Bond GM, Robertson IM, Birnbaum HK. The influence of hydrogen on deformation and fracture processes in high-strength aluminum alloys. Acta Metall 1987;35(9):2289–96. https://doi.org/10.1016/0001-6160(87)90076-9.
[11] Robertson IM, Birnbaum HK. An HVEM study of hydrogen effects on the deformation and fracture of nickel. Acta Metall 1986;34(3):353–66. https://doi.org/10.1016/0001-6160(86)90071-4.
[12] Tabata T, Birnbaum HK. Direct observations of the effect of hydrogen on the behavior of dislocations in iron. Scripta Metall 1983;17(7):947–50. https://doi.org/10.1016/0036-9748(83)90268-5.
[13] Beachem CD. A new model for hydrogen-assisted cracking (hydrogen "embrittlement"). Metall Mater Trans B 1972;3(2):441–55. https://doi.org/10.1007/BF02642048.
[14] Nagumo M, Ohta K, Saitoh H. Deformation induced defects in iron revealed by thermal desorption spectroscopy of tritium. Scripta Mater 1999;40(3):313–9. https://doi.org/10.1016/S1359-6462(98)00436-9.
[15] Hanley ES, Deane JP, Gallachóir BPÓ. The role of hydrogen in low carbon energy futures–A review of existing perspectives. Renew Sustain Energy Rev 2018;82:3027–45. https://doi.org/10.1016/j.rser.2017.10.034.
[16] Yue M, Lambert H, Pahon E, Roche R, Jemei S, Hissel D. Hydrogen energy systems: a critical review of technologies, applications, trends and challenges. Renew Sustain Energy Rev 2021;146:111180. https://doi.org/10.1016/j.rser.2021.111180.
[17] Sharma S, Ghoshal SK. Hydrogen the future transportation fuel: from production to applications. Renew Sustain Energy Rev 2015;43:1151–8. https://doi.org/10.1016/j.rser.2014.11.093.
[18] Usman MR. Hydrogen storage methods: review and current status. Renew Sustain Energy Rev 2022;167:112743. https://doi.org/10.1016/j.rser.2022.112743.
[19] Mazloomi K, Gomes C. Hydrogen as an energy carrier: prospects and challenges. Renew Sustain Energy Rev 2012;16(5):3024–33. https://doi.org/10.1016/j.rser.2012.02.028.
[20] Quarton CJ, Samsatli S. Power-to-gas for injection into the gas grid: what can we learn from real-life projects, economic assessments and systems modelling? Renew Sustain Energy Rev 2018;98:302–16. https://doi.org/10.1016/j.rser.2018.09.007.
[21] Tarkowski R. Underground hydrogen storage: characteristics and prospects. Renew Sustain Energy Rev 2019;105:86–94. https://doi.org/10.1016/j.rser.2019.01.051.
[22] Sdanghi G, Maranzana G, Celzard A, Fierro V. Review of the current technologies and performances of hydrogen compression for stationary and automotive applications. Renew Sustain Energy Rev 2019;102:150–70. https://doi.org/10.1016/j.rser.2018.11.028.
[23] Nagumo M, Takai K. The predominant role of strain-induced vacancies in hydrogen embrittlement of steels: overview. Acta Mater 2019;165:722–33. https://doi.org/10.1016/j.actamat.2018.12.013.
[24] Neeraj T, Srinivasan R, Li J. Hydrogen embrittlement of ferritic steels: observations on deformation microstructure, nanoscale dimples and failure by nanovoiding. Acta Mater 2012;60(13):5160–71. https://doi.org/10.1016/j.actamat.2012.06.014.
[25] Tehranchi A, Curtin WA. The role of atomistic simulations in probing hydrogen effects on plasticity and embrittlement in metals. Eng Fract Mech 2019;216:106502. https://doi.org/10.1016/j.engfracmech.2019.106502.
[26] Barrera O, Bombac D, Chen Y, Daff TD, Galindo-Nava E, Gong P, Haley D, Horton R, Katzarov I, Kermode JR, Liverani C, Stopher M, Sweeney F. Understanding and mitigating hydrogen embrittlement of steels: a review of experimental, modelling and design progress from atomistic to continuum. J Mater Sci 2018;53(9):6251–90. https://doi.org/10.1007/s10853-017-1978-5.
[27] Martin ML, Connolly MJ, DelRio FW, Slifka AJ. Hydrogen embrittlement in ferritic steels. Appl Phys Rev 2020;7(4):041301. https://doi.org/10.1063/5.0012851.
[28] Zhong W, Cai Y, Tománek D. Computer simulation of hydrogen embrittlement in metals. Nature 1993;362(6419):435–7. https://doi.org/10.1038/362435a0.
[29] Kresse G, Hafner J. Ab initio molecular dynamics for open-shell transition metals. Phys Rev B 1993;48(17):13115–8. https://doi.org/10.1103/PhysRevB.48.13115.
[30] Lu D, Wang H, Chen M, Lin L, Car R, E W, Jia W, Zhang L. 86 PFLOPS Deep Potential Molecular Dynamics simulation of 100 million atoms with ab initio accuracy. Comput Phys Commun 2021;259:107624. https://doi.org/10.1016/j.cpc.2020.107624.
[31] Wang H, Zhang L, Han J, DeePMD-kit WE. A deep learning package for many-body potential energy representation and molecular dynamics. Comput Phys Commun 2018;228:178–84. https://doi.org/10.1016/j.cpc.2018.03.016.
[32] Jia W, Wang H, Chen M, Lu D, Lin L, Car R, Weinan E, Zhang L. Pushing the limit of molecular dynamics with ab initio accuracy to 100 million atoms with machine learning. SC20: international conference for high performance computing, networking, storage and analysis. 2020. https://doi.org/10.1109/SC41405.2020.00009. Atlanta, GA, USA. 9-19 Nov.
[33] Yaghoobi M, Voyiadjis GZ. Size effects in fcc crystals during the high rate compression test. Acta Mater 2016;121:190–201. https://doi.org/10.1016/j.actamat.2016.09.010.
[34] Shibuta Y, Sakane S, Miyoshi E, Okita S, Takaki T, Ohno M. Heterogeneity in homogeneous nucleation from billion-atom molecular dynamics simulation of solidification of pure metal. Nat Commun 2017;8(1):10. https://doi.org/10.1038/s41467-017-00017-5.
[35] K. Nguyen-Cong, J.T. Willman, S.G. Moore, A.B. Belonoshko, R. Gayatri, E. Weinberg, M.A. Wood, A.P. Thompson, I.I. Oleynik. Billion atom molecular dynamics simulations of carbon at extreme conditions and experimental time and length scales. Proceedings of the International Conference for High Performance Computing, Networking, Storage and Analysis. St. Louis, Missouri. https://doi.org/10.1145/3458817.3487400.

[36] Cho L, Sulistiyo DH, Seo EJ, Jo KR, Kim SW, Oh JK, Cho YR, De Cooman BC. Hydrogen absorption and embrittlement of ultra-high strength aluminized press hardening steel. Mater Sci Eng, A 2018;734:416–26. https://doi.org/10.1016/j.msea.2018.08.003.
[37] Alvine KJ, Tyagi M, Brown C, Udovic TJ, Jenkins T, Pitman SG. Hydrogen species motion in piezoelectrics: a quasi-elastic neutron scattering study. J Appl Phys 2012;111(5):053505. https://doi.org/10.1063/1.3691114.
[38] Kimura A, Nakatani Y, Yamada K, Suzuki T. Elastic recoil detection analysis of hydrogen in high strength steel. J Mater Sci Lett 2000;19(11):965–6. https://doi.org/10.1023/A:1006768221947.
[39] Kesten P, Pundt A, Schmitz G, Weisheit M, Krebs HU, Kirchheim R. H- and D distribution in metallic multilayers studied by 3-dimensional atom probe analysis and secondary ion mass spectrometry. J Alloys Compd 2002;330–332:225–8. https://doi.org/10.1016/S0925-8388(01)01596-1.
[40] Takahashi J, Kawakami K, Kobayashi Y, Tarui T. The first direct observation of hydrogen trapping sites in TiC precipitation-hardening steel through atom probe tomography. Scripta Mater 2010;63(3):261–4. https://doi.org/10.1016/j.scriptamat.2010.03.012.
[41] Takahashi J, Kawakami K, Tarui T. Direct observation of hydrogen-trapping sites in vanadium carbide precipitation steel by atom probe tomography. Scripta Mater 2012;67(2):213–6. https://doi.org/10.1016/j.scriptamat.2012.04.022.
[42] Chen Y-S, Haley D, Bagot PAJ, Moody MP. Simplifying observation of hydrogen trapping in atom probe tomography. Microsc Microanal 2017;23(S1):620–1. https://doi.org/10.1017/S1431927617003774.
[43] Jiang YF, Zhang B, Zhou Y, Wang JQ, Han EH, Ke W. Atom probe tomographic observation of hydrogen trapping at carbides/ferrite interfaces for a high strength steel. J Mater Sci Technol 2018;34(8):1344–8. https://doi.org/10.1016/j.jmst.2017.11.008.
[44] Chen Y-S, Lu H, Liang J, Rosenthal A, Liu H, Sneddon G, McCarroll I, Zhao Z, Li W, Guo A, Cairney JM. Observation of hydrogen trapping at dislocations, grain boundaries, and precipitates. Science 2020;367(6474):171–5. https://doi.org/10.1126/science.aaz0122.
[45] Chen Y-S, Haley D, Gerstl SSA, London AJ, Sweeney F, Wepf RA, Rainforth WM, Bagot PAJ, Moody MP. Direct observation of individual hydrogen atoms at trapping sites in a ferritic steel. Science 2017;355(6330):1196–9. https://doi.org/10.1126/science.aal2418.
[46] Karnesky J, Richard A, Bartelt NC, Huang D, Teslich J, Nick E, Kumar M. Imaging and quantification of hydrogen isotope trapping. 2012. Albuquerque, NM, and Livermore, CA, SAND2012-8539.
[47] Zhao H, Chakraborty P, Ponge D, Hickel T, Sun B, Wu C-H, Gault B, Raabe D. Hydrogen trapping and embrittlement in high-strength Al alloys. Nature 2022;602(7897):437–41. https://doi.org/10.1038/s41586-021-04343-z.
[48] Zhang BL, Zhu QS, Xu C, Li CT, Ma Y, Ma ZX, Liu SN, Shao RW, Xu YT, Jiang BL, Gao L, Pang XL, He Y, Chen G, Qiao LJ. Atomic-scale insights on hydrogen trapping and exclusion at incoherent interfaces of nanoprecipitates in martensitic steels. Nat Commun 2022;13(1). https://doi.org/10.1038/s41467-022-31665-x.
[49] Hua Z, Zhu S, An B, Iijima T, Gu C, Zheng J. The finding of hydrogen trapping at phase boundary in austenitic stainless steel by scanning Kelvin probe force microscopy. Scripta Mater 2019;162:219–22. https://doi.org/10.1016/j.scriptamat.2018.11.020.
[50] Ma Z, Xiong X, Chen L, Su Y. Quantitative calibration of the relationship between Volta potential measured by scanning Kelvin probe force microscope (SKPFM) and hydrogen concentration. Electrochim Acta 2021;366:137422. https://doi.org/10.1016/j.electacta.2020.137422.
[51] Cheng B, Paxton AT, Ceriotti M. Hydrogen diffusion and trapping in α-iron: the role of quantum and anharmonic fluctuations. Phys Rev Lett 2018;120(22):225901. https://doi.org/10.1103/PhysRevLett.120.225901.
[52] Davidson E, Daff T, Csanyi G, Finnis M. Grand canonical approach to modeling hydrogen trapping at vacancies in α-Fe. Phys Rev Mater 2020;4(6):063804. https://doi.org/10.1103/PhysRevMaterials.4.063804.
[53] He Y, Li Y, Zhao X, Yu H, Chen C. Effect of hydrogen atom and hydrogen filled vacancies on stacking fault energy in γ-Fe by first-principles calculations. Int J Hydrogen Energy 2019;44(31):17136–45. https://doi.org/10.1016/j.ijhydene.2019.04.229.
[54] Di Stefano D, Mrovec M, Elsässer C. First-principles investigation of hydrogen trapping and diffusion at grain boundaries in nickel. Acta Mater 2015;98:306–12. https://doi.org/10.1016/j.actamat.2015.07.031.
[55] Song HY, Li CF, Geng SF, An MR, Xiao MX, Wang L. Atomistic simulations of effect of hydrogen atoms on mechanical behaviour of an α-Fe with symmetric tilt grain boundaries. Phys Lett 2018;382(35):2464–9. https://doi.org/10.1016/j.physleta.2018.06.005.
[56] Zhou X, Marchand D, McDowell DL, Zhu T, Song J. Chemomechanical origin of hydrogen trapping at grain boundaries in fcc metals. Phys Rev Lett 2016;116(7):075502. https://doi.org/10.1103/PhysRevLett.116.075502.
[57] Du YA, Ismer L, Rogal J, Hickel T, Neugebauer J, Drautz R. First-principles study on the interaction of H interstitials with grain boundaries in α- and γ-Fe. Phys Rev B 2011;84(14):144121. https://doi.org/10.1103/PhysRevB.84.144121.
[58] Tateyama Y, Ohno T. Stability and clusterization of hydrogen-vacancy complexes in α-Fe: an ab initio study. Phys Rev B 2003;67(17):174105. https://doi.org/10.1103/PhysRevB.67.174105.
[59] He Y, Li Y, Chen C, Yu H. Diffusion coefficient of hydrogen interstitial atom in α-Fe, γ-Fe and ε-Fe crystals by first-principle calculations. Int J Hydrogen Energy 2017;42(44):27438–45. https://doi.org/10.1016/j.ijhydene.2017.08.212.
[60] Hickel T, Nazarov R, McEniry EJ, Leyson G, Grabowski B, Neugebauer J. Ab initio based understanding of the segregation and diffusion mechanisms of hydrogen in steels. JOM 2014;66(8):1399–405. https://doi.org/10.1007/s11837-014-1055-3.
[61] Momida H, Asari Y, Nakamura Y, Tateyama Y, Ohno T. Hydrogen-enhanced vacancy embrittlement of grain boundaries in iron. Phys Rev B 2013;88(14):144107. https://doi.org/10.1103/PhysRevB.88.144107.
[62] Monasterio PR, Lau TT, Yip S, Van Vliet KJ. Hydrogen-vacancy interactions in Fe-C alloys. Phys Rev Lett 2009;103(8):085501. https://doi.org/10.1103/PhysRevLett.103.085501.
[63] Becquart CS, Domain C. Solute–point defect interactions in bcc systems: focus on first principles modelling in W and RPV steels. Curr Opin Solid State Mater Sci 2012;16(3):115–25. https://doi.org/10.1016/j.cossms.2012.01.001.
[64] Samin AJ, Andersson DA, Holby EF, Uberuaga BP. First-principles localized cluster expansion study of the kinetics of hydrogen diffusion in homogeneous and heterogeneous Fe-Cr alloys. Phys Rev B 2019;99(1):014110. https://doi.org/10.1103/PhysRevB.99.014110.
[65] Counts WA, Wolverton C, Gibala R. First-principles energetics of hydrogen traps in α-Fe: point defects. Acta Mater 2010;58(14):4730–41. https://doi.org/10.1016/j.actamat.2010.05.010.
[66] Zhou X, Curtin WA. First principles study of the effect of hydrogen in austenitic stainless steels and high entropy alloys. Acta Mater 2020;200:932–42. https://doi.org/10.1016/j.actamat.2020.09.070.
[67] Sofronis P, Liang Y, Aravas N. Hydrogen induced shear localization of the plastic flow in metals and alloys. Eur J Mech Solid 2001;20(6):857–72. https://doi.org/10.1016/S0997-7538(01)01179-2.
[68] Katzarov IH, Pashov DL, Paxton AT. Hydrogen embrittlement I. Analysis of hydrogen-enhanced localized plasticity: effect of hydrogen on the velocity of screw dislocations in α-Fe. Phys Rev Mater 2017;1(3):033602. https://doi.org/10.1103/PhysRevMaterials.1.033602.
[69] McEniry EJ, Hickel T, Neugebauer J. Ab initio simulation of hydrogen-induced decohesion in cementite-containing microstructures. Acta Mater 2018;150:53–8. https://doi.org/10.1016/j.actamat.2018.03.005.
[70] Echeverri Restrepo S, Di Stefano D, Mrovec M, Paxton AT. Density functional theory calculations of iron - vanadium carbide interfaces and the effect of hydrogen. Int J Hydrogen Energy 2020;45(3):2382–9. https://doi.org/10.1016/j.ijhydene.2019.11.102.
[71] Ma Y, Shi Y, Wang H, Mi Z, Liu Z, Gao L, Yan Y, Su Y, Qiao L. A first-principles study on the hydrogen trap characteristics of coherent nano-precipitates in α-Fe. Int J Hydrogen Energy 2020;45(51):27941–9. https://doi.org/10.1016/j.ijhydene.2020.07.123.
[72] Liu Y, Huang S, Ding J, Yang Y, Zhao J. Vanadium carbide coating as hydrogen permeation barrier: a DFT study. Int J Hydrogen Energy 2019;44(12):6093–102. https://doi.org/10.1016/j.ijhydene.2019.01.049.
[73] Sun Y, Cheng YF. Thermodynamics of spontaneous dissociation and dissociative adsorption of hydrogen molecules and hydrogen atom adsorption and absorption on steel under pipelining conditions. Int J Hydrogen Energy 2021;46(69):34469–86. https://doi.org/10.1016/j.ijhydene.2021.07.217.
[74] Sanchez J, Ridruejo A, de Andres PL. Diffusion and trapping of hydrogen in carbon steel at different temperatures. Theor Appl Fract 2020;110:102803. https://doi.org/10.1016/j.tafmec.2020.102803.
[75] Gunaydin H, Barabash SV, Houk KN, Ozolins V. First-principles theory of hydrogen diffusion in aluminum. Phys Rev Lett 2008;101(7):075901. https://doi.org/10.1103/PhysRevLett.101.075901.
[76] Meng F-S, Du J-P, Shinzato S, Mori H, Yu P, Matsubara K, Ishikawa N, Ogata S. General-purpose neural network interatomic potential for the α-iron and hydrogen binary system: toward atomic-scale understanding of hydrogen embrittlement. Phys Rev Mater 2021;5(11):113606. https://doi.org/10.1103/PhysRevMaterials.5.113606.
[77] Lee B-J, Jang J-W. A modified embedded-atom method interatomic potential for the Fe–H system. Acta Mater 2007;55(20):6779–88. https://doi.org/10.1016/j.actamat.2007.08.041.
[78] Ramasubramaniam A, Itakura M, Carter EA. Interatomic potentials for hydrogen in α-iron based on density functional theory. Phys Rev B 2009;79(17):174101. https://doi.org/10.1103/PhysRevB.79.174101.
[79] Starikov S, Smirnova D, Pradhan T, Lysogorskiy Y, Chapman H, Mrovec M, Drautz R. Angular-dependent interatomic potential for large-scale atomistic simulation of iron: development and comprehensive comparison with existing interatomic models. Phys Rev Mater 2021;5(6):063607. https://doi.org/10.1103/PhysRevMaterials.5.063607.
[80] Apostol F, Mishin Y. Angular-dependent interatomic potential for the aluminum-hydrogen system. Phys Rev B 2010;82(14):144115. https://doi.org/10.1103/PhysRevB.82.144115.
[81] Zhou XW, Ward DK, Foster ME. A bond-order potential for the Al–Cu–H ternary system. New J Chem 2018;42(7):5215–28. https://doi.org/10.1039/C8NJ00513C.
[82] Goryaeva AM, Dérès J, Lapointe C, Grigorev P, Swinburne TD, Kermode JR, Ventelon L, Baima J, Marinica M-C. Efficient and transferable machine learning potentials for the simulation of crystal defects in bcc Fe and W. Phys Rev Mater 2021;5(10):103803. https://doi.org/10.1103/PhysRevMaterials.5.103803.
[83] Wang X, Xu S, Jian W-R, Li X-G, Su Y, Beyerlein IJ. Generalized stacking fault energies and Peierls stresses in refractory body-centered cubic metals from machine learning-based interatomic potentials. Comput Mater Sci 2021;192:110364. https://doi.org/10.1016/j.commatsci.2021.110364.
[84] Xing X, Yu M, Chen W, Zhang H. Atomistic simulation of hydrogen-assisted ductile-to-brittle transition in α-iron. Comput Mater Sci 2017;127:211–21. https://doi.org/10.1016/j.commatsci.2016.10.033.
[85] Wang Z, Shi X, Yang X-S, He W, Shi S-Q, Ma X. Atomistic simulation of the effect of the dissolution and adsorption of hydrogen atoms on the fracture of α-Fe single

crystal under tensile load. Int J Hydrogen Energy 2021;46(1):1347–61. https://doi.org/10.1016/j.ijhydene.2020.09.216.
[86] Song J, Curtin WA. Atomic mechanism and prediction of hydrogen embrittlement in iron. Nat Mater 2013;12(2):145–51. https://doi.org/10.1038/nmat3479.
[87] Xing X, Zhang Y, Wang S, Li Z, Yang C, Cui G, Zhang S, Liu J, Gou J, Yu H. Atomistic simulation of hydrogen-induced plastic zone compression during cyclic loading. Int J Hydrogen Energy 2020;45(31):15697–709. https://doi.org/10.1016/j.ijhydene.2020.04.062.
[88] White PD, Barter SA, Medhekar N. Hydrogen induced amorphisation around nanocracks in aluminium. Eng Fract Mech 2016;161:40–54. https://doi.org/10.1016/j.engfracmech.2016.04.024.
[89] Yu P, Cui Y, Zhu G-z, Shen Y, Wen M. The key role played by dislocation core radius and energy in hydrogen interaction with dislocations. Acta Mater 2020;185:518–27. https://doi.org/10.1016/j.actamat.2019.12.033.
[90] Nowak C, Sills RB, Ronevich JA, San Marchi CW, Zhou XW. Atomistic simulations of hydrogen distribution in Fe–C steels. Int J Hydrogen Energy 2022;47(76):32732–40. https://doi.org/10.1016/j.ijhydene.2022.07.166.
[91] Zhu Y, Li Z, Huang M, Fan H. Study on interactions of an edge dislocation with vacancy-H complex by atomistic modelling. Int J Plast 2017;92:31–44. https://doi.org/10.1016/j.ijplas.2017.03.003.
[92] Bao Q, Huang M, Zhu Y, Zhao L, Li Z. Abnormal interactions between high-speed edge dislocation and microvoid in BCC metals. Int J Plast 2022;148:103125. https://doi.org/10.1016/j.ijplas.2021.103125.
[93] Zhou X, Ouyang B, Curtin WA, Song J. Atomistic investigation of the influence of hydrogen on dislocation nucleation during nanoindentation in Ni and Pd. Acta Mater 2016;116:364–9. https://doi.org/10.1016/j.actamat.2016.06.061.
[94] Zhao K, He J, Mayer AE, Zhang Z. Effect of hydrogen on the collective behavior of dislocations in the case of nanoindentation. Acta Mater 2018;148:18–27. https://doi.org/10.1016/j.actamat.2018.01.053.
[95] Yavas D, Phan T, Xiong L, Hebert KR, Bastawros AF. Mechanical degradation due to vacancies produced by grain boundary corrosion of steel. Acta Mater 2020;200:471–80. https://doi.org/10.1016/j.actamat.2020.08.080.
[96] Wang S, Martin ML, Robertson IM, Sofronis P. Effect of hydrogen environment on the separation of Fe grain boundaries. Acta Mater 2016;107:279–88. https://doi.org/10.1016/j.actamat.2016.01.067.
[97] Ding Y, Yu H, Lin M, Zhao K, Xiao S, Vinogradov A, Qiao L, Ortiz M, He J, Zhang Z. Hydrogen-enhanced grain boundary vacancy stockpiling causes transgranular to intergranular fracture transition. Acta Mater 2022;239:118279. https://doi.org/10.1016/j.actamat.2022.118279.
[98] Li J, Lu C, Pei L, Zhang C, Wang R, Tieu K. Effects of H segregation on shear-coupled motion of <110> grain boundaries in α-Fe. Int J Hydrogen Energy 2019;44(33):18616–27. https://doi.org/10.1016/j.ijhydene.2019.05.071.
[99] Zhang S, Zhao Q, Liu J, Huang F, Huang Y, Li X. Understanding the effect of niobium on hydrogen-induced blistering in pipeline steel: a combined experimental and theoretical study. Corrosion Sci 2019;159:108142. https://doi.org/10.1016/j.corsci.2019.108142.
[100] Qu J, Feng M, An T, Bi Z, Du J, Yang F, Zheng S. Hydrogen-assisted crack growth in the heat-affected zone of X80 steels during in situ hydrogen charging. Materials 2019;12(16):2575. https://doi.org/10.3390/ma12162575.
[101] Wang X, Zhao Y, Cheng G, Zhang Y, Venkatesh TA. Hydrogen adsorption in phase and grain boundaries of pearlitic steels and its effects on tensile strength. MRS Adv 2022;7:383–7. https://doi.org/10.1557/s43580-022-00237-y.
[102] Zhu Y, Li Z, Huang M. Solute hydrogen effects on plastic deformation mechanisms of α-Fe with twist grain boundary. Int J Hydrogen Energy 2018;43(22):10481–95. https://doi.org/10.1016/j.ijhydene.2018.04.133.
[103] Chen J, Zhu Y, Huang M, Zhao L, Liang S, Li Z. Study on hydrogen-affected interaction between dislocation and grain boundary by MD simulation. Comput Mater Sci 2021;196:110562. https://doi.org/10.1016/j.commatsci.2021.110562.
[104] Li J, Lu C, Pei L, Zhang C, Wang R. Hydrogen-modified interaction between lattice dislocations and grain boundaries by atomistic modelling. Int J Hydrogen Energy 2020;45(15):9174–87. https://doi.org/10.1016/j.ijhydene.2020.01.103.
[105] Kapci MF, Schön JC, Bal B. The role of hydrogen in the edge dislocation mobility and grain boundary-dislocation interaction in α-Fe. Int J Hydrogen Energy 2021;46(64):32695–709. https://doi.org/10.1016/j.ijhydene.2021.07.061.
[106] Wan L, Geng WT, Ishii A, Du J-P, Mei Q, Ishikawa N, Kimizuka H, Ogata S. Hydrogen embrittlement controlled by reaction of dislocation with grain boundary in alpha-iron. Int J Plast 2019;112:206–19. https://doi.org/10.1016/j.ijplas.2018.08.013.
[107] Ramasubramaniam A, Itakura M, Carter EA. Interatomic potentials for hydrogen in α–iron based on density functional theory. Phys Rev B 2009;79(17):174101. https://doi.org/10.1103/PhysRevB.79.174101.
[108] O'Brien C, Foiles SM. Hydrogen segregation to inclined Σ3⟨1 1 0⟩ twin grain boundaries in nickel. Philos Mag A 2016;96(26):2808–28. https://doi.org/10.1080/14786435.2016.1217094.
[109] Li J, Lu C, Pei L, Zhang C, Wang R. Atomistic investigation of hydrogen induced decohesion of Ni grain boundaries. Mech Mater 2020;150:103586. https://doi.org/10.1016/j.mechmat.2020.103586.
[110] Zheng Y, Yu P, Zhang K, Wen M, Zheng J, Zhou C, Zhang L. Coupling effect of grain boundary and hydrogen segregation on dislocation nucleation in bi-crystal nickel. Int J Hydrogen Energy 2020;45(38):20021–31. https://doi.org/10.1016/j.ijhydene.2020.04.291.
[111] Ding Y, Yu H, Zhao K, Lin M, Xiao S, Ortiz M, He J, Zhang Z. Hydrogen-induced transgranular to intergranular fracture transition in bi-crystalline nickel. Scripta Mater 2021;204:114122. https://doi.org/10.1016/j.scriptamat.2021.114122.
[112] Barrows W, Dingreville R, Spearot D. Traction–separation relationships for hydrogen induced grain boundary embrittlement in nickel via molecular dynamics simulations. Mater Sci Eng, A 2016;650:354–64. https://doi.org/10.1016/j.msea.2015.10.042.
[113] Tehranchi A, Zhou X, Curtin WA. A decohesion pathway for hydrogen embrittlement in nickel: mechanism and quantitative prediction. Acta Mater 2020;185:98–109. https://doi.org/10.1016/j.actamat.2019.11.062.
[114] Harris ZD, Lawrence SK, Medlin DL, Guetard G, Burns JT, Somerday BP. Elucidating the contribution of mobile hydrogen-deformation interactions to hydrogen-induced intergranular cracking in polycrystalline nickel. Acta Mater 2018;158:180–92. https://doi.org/10.1016/j.actamat.2018.07.043.
[115] Lawrence SK, Yagodzinskyy Y, Hänninen H, Korhonen E, Tuomisto F, Harris ZD, Somerday BP. Effects of grain size and deformation temperature on hydrogen-enhanced vacancy formation in Ni alloys. Acta Mater 2017;128:218–26. https://doi.org/10.1016/j.actamat.2017.02.016.
[116] Tigli A, Sahin H, Dizdar KC, Dispinar D. Determination of effect of hydrogen on strength of aluminum by MD simulation. Appl Phys A 2022;128(9):822. https://doi.org/10.1007/s00339-022-05981-4.
[117] Zhou X-Y, Yang X-S, Zhu J-H, Xing F. Atomistic simulation study of the grain-size effect on hydrogen embrittlement of nanograined Fe. Int J Hydrogen Energy 2020;45(4):3294–306. https://doi.org/10.1016/j.ijhydene.2019.11.131.
[118] Ramunni VP, Pascuet MI, Castin N, Rivas AMF. The influence of grain size on the hydrogen diffusion in bcc Fe. Comput Mater Sci 2021;188:110146. https://doi.org/10.1016/j.commatsci.2020.110146.
[119] Zhou X-Y, Zhu J-H, Wu H-H, Yang X-S, Wang S, Mao X. Unveiling the role of hydrogen on the creep behaviors of nanograined α-Fe via molecular dynamics simulations. Int J Hydrogen Energy 2021;46(14):9613–29. https://doi.org/10.1016/j.ijhydene.2020.12.115.
[120] Koyama M, Taheri-Mousavi SM, Yan H, Kim J, Cameron BC, Moeini-Ardakani SS, Li J, Tasan CC. Origin of micrometer-scale dislocation motion during hydrogen desorption. Sci Adv 2020;6(23):eaaz1187. https://doi.org/10.1126/sciadv.aaz1187.
[121] Zhou XW, Foster ME, Sills RB. An Fe-Ni-Cr embedded atom method potential for austenitic and ferritic systems. J Comput Chem 2018;39(29):2420–31. https://doi.org/10.1002/jcc.25573.
[122] Zhou XW, Nowak C, Skelton RS, Foster ME, Ronevich JA, San Marchi C, Sills RB. An Fe-Ni-Cr-H interatomic potential and predictions of hydrogen-affected stacking fault energies in austenitic stainless steels. Int J Hydrogen Energy 2022;47(1):651–65. https://doi.org/10.1016/j.ijhydene.2021.09.261.
[123] Turk A, Pu SD, Bombač D, Rivera-Díaz-del-Castillo PEJ, Galindo-Nava EI. Quantification of hydrogen trapping in multiphase steels: Part II – effect of austenite morphology. Acta Mater 2020;197:253–68. https://doi.org/10.1016/j.actamat.2020.07.039.
[124] Hussein A, Krom AHM, Dey P, Sunnardianto GK, Moultos OA, Walters CL. The effect of hydrogen content and yield strength on the distribution of hydrogen in steel: a diffusion coupled micromechanical FEM study. Acta Mater 2021;209:116799. https://doi.org/10.1016/j.actamat.2021.116799.
[125] Anand L, Mao Y, Talamini B. On modeling fracture of ferritic steels due to hydrogen embrittlement. J Mech Phys Solid 2019;122:280–314. https://doi.org/10.1016/j.jmps.2018.09.012.
[126] Golahmar A, Kristensen PK, Niordson CF, Martínez-Pañeda E. A phase field model for hydrogen-assisted fatigue. Int J Fatig 2022;154:106521. https://doi.org/10.1016/j.ijfatigue.2021.106521.
[127] Gu Y, El-Awady JA. Quantifying the effect of hydrogen on dislocation dynamics: a three-dimensional discrete dislocation dynamics framework. J Mech Phys Solid 2018;112:491–507. https://doi.org/10.1016/j.jmps.2018.01.006.
[128] Yu H, Cocks A, Tarleton E. Discrete dislocation plasticity HELPs understand hydrogen effects in bcc materials. J Mech Phys Solid 2019;123:41–60. https://doi.org/10.1016/j.jmps.2018.08.020.
[129] Charles Y, Nguyen HT, Gaspérini M. Comparison of hydrogen transport through pre-deformed synthetic polycrystals and homogeneous samples by finite element analysis. Int J Hydrogen Energy 2017;42(31):20336–50. https://doi.org/10.1016/j.ijhydene.2017.06.016.
[130] Drexler A, Depover T, Verbeken K, Ecker W. Model-based interpretation of thermal desorption spectra of Fe-C-Ti alloys. J Alloys Compd 2019;789:647–57. https://doi.org/10.1016/j.jallcom.2019.03.102.
[131] Martínez-Pañeda E, Golahmar A, Niordson CF. A phase field formulation for hydrogen assisted cracking. Comput Methods Appl Mech Eng 2018;342:742–61. https://doi.org/10.1016/j.cma.2018.07.021.
[132] Arnaudov N, Kolyshkin A, Weihe S. Micromechanical modeling of fatigue crack initiation in hydrogen atmosphere. Mech Mater 2020;149:103557. https://doi.org/10.1016/j.mechmat.2020.103557.
[133] Valverde-González A, Martínez-Pañeda E, Quintanas-Corominas A, Reinoso J, Paggi M. Computational modelling of hydrogen assisted fracture in polycrystalline materials. Int J Hydrogen Energy 2022;47(75):32235–51. https://doi.org/10.1016/j.ijhydene.2022.07.117.
[134] San Marchi C, Ronevich JA. Fatigue and fracture of pipeline steels in high-pressure hydrogen gas. ASME 2022 pressure vessels & piping conference. Nevada, USA: Las Vegas; 2022. https://doi.org/10.1115/PVP2022-84757. July 17–22.
[135] Kagay B, Ronevich J, San Marchi C. Influence of high-pressure hydrogen gas and pre-charged hydrogen on fatigue crack initiation and fatigue life of 255 super duplex stainless steel. ASME 2022 pressure vessels & piping conference. Nevada, USA: Las Vegas; 2022. https://doi.org/10.1115/pvp2022-84797. July 17–22.
[136] Emery JM, Grimmer P, Wheeler III R, San Marchi C, Ronevich J. Fatigue design sensitivities of stationary type 2 high-pressure hydrogen vessels. ASME 2022 pressure vessels & piping conference. Nevada, USA: Las Vegas; 2022. https://doi.org/10.1115/PVP2022-83904. July 17–22.

[137] Marchi CS, Ronevich J. Design and operation of metallic pipelines for service in hydrogen and blends. 2022. Livermore, CA, USA, SAND2022-8369 PE.
[138] Sudmanns M, El-Awady JA. The effect of local chemical ordering on dislocation activity in multi-principle element alloys: a three-dimensional discrete dislocation dynamics study. Acta Mater 2021;220:117307. https://doi.org/10.1016/j.actamat.2021.117307.
[139] Hart GLW, Mueller T, Toher C, Curtarolo S. Machine learning for alloys. Nat Rev Mater 2021;6(8):730–55. https://doi.org/10.1038/s41578-021-00340-w.
[140] Taylor CD, Lu P, Saal J, Frankel GS, Scully JR. Integrated computational materials engineering of corrosion resistant alloys. NPJ Mater Degrad 2018;2(1):6. https://doi.org/10.1038/s41529-018-0027-4.
[141] Curtarolo S, Hart GLW, Nardelli MB, Mingo N, Sanvito S, Levy O. The high-throughput highway to computational materials design. Nat Mater 2013;12(3):191–201. https://doi.org/10.1038/nmat3568.
[142] Rodenkirchen C, Appleton M, Ryan MP, Pedrazzini S. A review on atom probe and correlative microscopy studies of corrosion in nickel-based superalloys. MRS Bull 2022;47(7):706–17. https://doi.org/10.1557/s43577-022-00366-7.
[143] Wang D, Lu X, Deng Y, Guo X, Barnoush A. Effect of hydrogen on nanomechanical properties in Fe-22Mn-0.6C TWIP steel revealed by in-situ electrochemical nanoindentation. Acta Mater 2019;166:618–29. https://doi.org/10.1016/j.actamat.2018.12.055.
[144] Cheng G, Choi KS, Hu X, Sun X. Determining individual phase properties in a multi-phase Q&P steel using multi-scale indentation tests. Mater Sci Eng, A 2016;652:384–95. https://doi.org/10.1016/j.msea.2015.11.072.
[145] Ronchi MR, Yan H, Tasan CC. Hydrogen-induced martensitic transformation and twinning in $Fe_{45}Mn_{35}Cr_{10}Co_{10}$. Metall Mater Trans A 2022;53(2):432–48. https://doi.org/10.1007/s11661-021-06498-w.
[146] Mine Y, Horita Z, Murakami Y. Effect of hydrogen on martensite formation in austenitic stainless steels in high-pressure torsion. Acta Mater 2009;57(10):2993–3002. https://doi.org/10.1016/j.actamat.2009.03.006.
[147] Solheim KG, Solberg JK, Walmsley J, Rosenqvist F, Bjørnå TH. The role of retained austenite in hydrogen embrittlement of supermartensitic stainless steel. Eng Fail Anal 2013;34:140–9. https://doi.org/10.1016/j.engfailanal.2013.07.025.
[148] Choi KS, Liu WN, Sun X, Khaleel MA. Microstructure-based constitutive modeling of TRIP steel: prediction of ductility and failure modes under different loading conditions. Acta Mater 2009;57(8):2592–604. https://doi.org/10.1016/j.actamat.2009.02.020.
[149] Gong P, Nutter J, Rivera-Diaz-Del-Castillo PEJ, Rainforth WM. Hydrogen embrittlement through the formation of low-energy dislocation nanostructures in nanoprecipitation-strengthened steels. Sci Adv 2020;6(46):abb6152. https://doi.org/10.1126/sciadv.abb6152.